The copyright of this thesis vests in the author. No quotation from it or information derived from it is to be published without full acknowledgement of the source. The thesis is to be used for private study or non-commercial research purposes only.

Published by the University of Cape Town (UCT) in terms of the non-exclusive license granted to UCT by the author.

University of Cape Town

THE EFFECT OF BOUNDARY CONDITIONS ON THE FAILURE OF THIN PLATES SUBJECTED TO IMPULSIVE LOADING.

by

B.M.THOMAS

1995

Submitted to the University of Cape Town as partial fulfilment of the degree of M.Sc in Mechanical engineering.

[illegible] Town has been given [illegible] in whole [illegible] by the author.

ACKNOWLEDGEMENTS

I would like to thank my supervisor Associate Professor G.N.Nurick for proposing the topic and for his interest, encouragement, and guidance.

I would also like to thank Mr M.Batho and the workshop staff for their help and advice, and Mr John Fitton for helping with the photography.

SYNOPSIS

This report presents the results of an investigation into the effects of edge boundary conditions on the failure of thin plates subjected to impulsive loading. In previous investigations the discrepancy between experimental results and theoretical solutions and effects observed at the edges of deformed plates have brought the method of securing the plate into question. This investigation examines the effect of edge boundary conditions by comparing the results of previous experiments - where the plates were secured by clamping - with experiments where the plates are built-in (integral) with their supports.

The specific objectives were to investigate the effects of edge boundary conditions and to establish the validity of previous results and theoretical solutions.

In the experiments both circular and square plates were investigated. The experimental method used was, with the exception of the method used to secure the plate, identical to that used in previous experiments. Explosive was used to generate the impulsive load and the plates were mounted on a ballistic pendulum in order to measure the impulse. The test plates used were machined from thick steel plates which were mounted on the pendulum so that the plates would be integral with their supports, thus forming a different, and more restrictive edge boundary.

The results showed that the results of previous experiments using clamps to secure

the plates are valid for mode I failure (deformation only), but NOT valid for predicting mode II failure (tearing). Mode II failure was shown to be dependent on a shear component for integral plates. Theoretical predictions which considered shear, successfully predicted mode II failure, whereas those that did not failed to.

The investigation identified differences between the clamped and integral plates at or near the edge boundary which influences the onset of mode II failure. Significantly, deformation occurs within the clamped region of the plate.

CONTENTS

LIST OF FIGURES

LIST OF TABLES

GLOSSARY

List of Terms

Built-in plate	Plate where the plate is built into the support.
Clamped plate	Plate which is fixed by clamping it to the support.
Integral plate	Another term used to describe the built-in plate.
Loaded side	Refers to the side of the plate that was loaded -the concave side of the plate.
Mode I failure	Failure resulting in large inelastic deformation of the plate.
Mode I(a) failure	Mode I failure at impulses below the necking point.
Mode I(b) failure	Mode I failure at impulses above the necking point.
Mode II failure	Failure resulting in inelastic deformation and rupture at the edge of the plate.
Mode III failure	Failure resulting in transverse shear failure at the support and little or no deformation.
Unloaded side	Refers to the side of the plate that was not loaded -the convex side of the plate.

Notation

Upper case

B Width of quadrangular plate, interchangeable with L for square plates.

D Material constant in the Cowper-Symonds constitutive equation.

I Impulse

I* Dimensionless impulse used by Shen and Jones [5].

L Length of quadrangular plate, interchangeable with B for square plates.

R Radius of circular plates.

R_o Radius of area over which the impulse is applied to circular plates.

Lower case

t Thickness of the plate

Greek Characters

δ_f Final deformation

ϵ_a Membrane strain

ϵ_b Bending strain

ϵ_f Failure Strain

ρ Density of material

σ_o Static yield stress

ϕ Damage number

$\phi_{c,s,q}$ Damage number for circular, square and Quadrangular plates.

1. INTRODUCTION

1.1. Motivation for the investigation

The investigation into the failure of thin plates subjected to impulsive loading has been on going for some years as reported by Nurick and Martin [1]. The failure of thin plates is important as a model of engineering structures undergoing large plastic deformations under dynamic loads.

In previous experimental work on the deformation and tearing of thin circular and rectangular plates restrained at the edges and subjected to impulsive loading, the edges have been restrained by clamping a thin plate between two thick plates with the appropriate shape cut out. Teeling-Smith and Nurick [2], in experiments investigating the failure of thin circular plates, observed evidence of radial movement in the clamped portion of the plate. Nurick and Teeling-Smith [3] defined necking at the plate edges of clamped circular plates which was investigated by Marshall [4]. Both this 'radial slip', and necking question whether the clamping method used can accurately produce a fully restrained boundary condition.

The observed radial slip is supported by Shen and Jones [5] as a possible reason for poor correlation between the predicted threshold of rupture and the experimental results of Teeling-Smith and Nurick [2] despite good correlation for mode I (deformation only) failure. Further experimental results were required, with attention given to details of the edge boundary conditions.

In previous experiments three modes of failure were identified:-

Mode I - large inelastic deformation

Mode II - tearing (tensile failure) at outer fibres, at or over the support

Mode III- transverse shear failure at the support [2]

It remained to be seen whether these modes would be present and in the same form, if the edges were restrained by a different method.

1.2. Objectives of the investigation

The objects of the investigation were:

1. To investigate the effects of edge boundary conditions on results of experiments examining the failure of thin plates subject to impulsive loading.
2. To determine the validity of the results, and empirical relations derived from previous experiments using different methods of restraining the plate edges.
3. To determine the validity of theoretical solutions.

1.3. Scope and limitations of the investigation

The scope of the investigation was limited to square and circular plates of fixed dimensions. The machining process, although very carefully monitored, did not

produce plates of consistently similar thickness. This was due to cutter wear and cumulative machining inaccuracies. This, however, had the rather serendipitous effect of demonstrating the influence of thickness on the results. Also as a result of the machining, the plate sections may not have been as smooth or have as consistent a thickness over the whole surface as would be the case for the plates used in experiments where the plate was clamped.

These affects would conspire to create an additional source of experimental scatter. This however should not be too significant compared with scatter caused by the difficult loading conditions involving explosives.

1.4. About this report

The information on which this report is based was gathered by means of a search in the available literature and from a series of experiments undertaken.

This report begins by defining the problem in chapter 2. In chapter 3 it discusses the results of the literature survey which covers previous theoretical work as well as experimental results and observations. Previous theory includes predictions of deflection and impact to failure. Previous experimental work is introduced for comparison with the results of this investigation. Observations of radial slip and necking, and investigations into necking are cited.

The experimental investigation is described in chapter 4, while the experimental

results are given in chapter 5. These results include tables of the data, photographs of the deformed plates and observations made.

In chapter 6 the results are compared with other experimental results and theoretical solutions. The comparison includes discussion of the results and the comparison with previous work. Finally conclusions are drawn and recommendations made in chapters 7 and 8 respectively.

2. PROBLEM STATEMENT

The problem can be stated as :

How does the edge boundary condition affect the failure of thin plates subjected to impulsive loading? In particular: How are the results affected by changing the method of restraining the edges? Does this affect correlation with theoretical solutions? And, are previous results valid and if not in what way must they be revised ?

3. LITERATURE SURVEY

Several attempts have been made in the past to theoretically predict the mid-point deflection / deflection-thickness ratio for thin plates subjected to impulsive loading, a review of these has been done by Nurick and Martin [1].

In addition there are some attempts to predict initiation of failure modes II (tearing) and III (shear). The ones referenced here are by Shen and Jones [5] and Jones [6,7] for fully clamped circular plates, and by Olson, Nurick and Fagnan [8] and Jones [6,9] for square plates.

Experimental results are perhaps more useful in these comparisons. A review by Nurick and Martin [1] is comprehensive in comparing many previous reports. Also used are the results of Teeling-Smith and Nurick [2], Nurick [10], Nurick and Teeling-Smith [3] and Olson, Nurick and Fagnan [8].

It is convenient to cover the literature in two sections, the first concerning theoretical solutions, the second concerning results from other experiments and empirical solutions.

3.1. Theoretical Solutions

The review by Nurick and Martin [1] gives a comprehensive overview of theoretical solutions and shows the wide range of solutions.

3.1.1. Circular Plates

The results of the experiments show that the effect of boundary conditions on the deformation of circular plates is small. This will be presented later, but here it is sufficient to state that the results are similar enough to previous experimental investigations that the results of previous correlations between theoretical and experimental deflections would still be valid.Thus comparisons between the results of this investigation and theoretical predictions have been limited to include only the work by Shen and Jones [5] and Jones [6,7].

Shen and Jones [5] present an approximate theoretical analysis into the deformation and rupture of fully clamped circular plates. The analysis combines bending moments, membrane force *and* transverse shear force and uses the Cowper-Symonds constitutive equation to include strain rate effects. There was good agreement with experimental results for permanent mid-point deflection. However the theoretical impulse to rupture ($I^* = 0.835$) was little more than half that found experimentally by Teeling-Smith and Nurick ($I^* = 1.52$)[2]. Shen and Jones suggest non-ideal boundary conditions as a possible reason for the poor correlation of impulse to rupture.

Shen and Jones [5] also demonstrated decreasing stiffness with increasing impulse between their theoretical prediction and experiments where plates were clamped to prevent rotation but allowed radial displacement. This suggests that when radial slip is occurring, the plate becomes less stiff and the deflection versus impulse

graph should diverge from the ideal non-slip graph. This information will be used later to show that the behaviour of clamped plates at impulses above the necking point is consistent with there being less radial restraint at the plate edge. Conversely this predicts that if through necking the plate is thinner, and thus not as securely constrained radially near the boundary, then the plate should behave as one less stiff.

Jones [6,7] presents an approximate theoretical procedure which includes strain rate effects to predict deflection.

$$(\frac{\delta_f}{t})=\sqrt{\frac{2}{3n}}\ \Phi \qquad \text{[6:equ. 8.88]}$$

where **n** introduces the effect of strain rate and is given by

$$n=1+(\frac{I^2}{48DR^5t^2\sqrt{3\sigma_o}\ \rho^{3/2}})^{1/q} \qquad \text{[6:equ. 8.89]}$$

and

$$\Phi=\frac{I}{\pi Rt^2(\rho\sigma_o)^{1/2}}$$

Jones' prediction of mode II failure uses the predicted deformation as discussed above and a prediction of strain based on the deformation.

$$\epsilon_f=2\{(\frac{\delta_f}{t})^2+\frac{R}{t}-1\}(\frac{t}{2R})^2 \qquad \text{[6:eqn. 7.140]}$$

The impulse to rupture is predicted as that required to cause strain that is greater or equal to the rupture stain of the material. Thus:-

$$\Phi=\sqrt{\frac{3n}{2}}\sqrt{\frac{\epsilon_f}{2}(\frac{2R}{t})^2+1}-\frac{R}{t}$$

Jones includes only bending and membrane strain.

3.1.2. Square Plates

Less theoretical work has been presented on the deformation and rupture of square plates than for circular plates. This can be attributed to the more complex nature of the quadrangular plate problem.

Jones [6] presents an approximate theoretical procedure which includes strain rate effects to predict deflection.

$$(\frac{\delta_f}{t})=(1+\Gamma/n)^{1/2}-1 \qquad \text{[6:equ. 8.90]}$$

where n introduces the effect of strain rate and is given by

$$n=1+(\frac{I^2}{\frac{3}{2}DL^5t^2\sqrt{3\sigma_o}\rho^{3/2}})^{1/q} \qquad \text{[6:equ. 8.92b]}$$

and

$$\Gamma=\frac{I^2}{6\rho\sigma_0L^2t^4} \qquad \text{[6:eqn. 8.91a]}$$

This procedure gives a lower bound for the deflection-thickness ratio. An upper bound can be found by replacing σ with 0.618 * σ_o. The constant 0.618 relates to the inscribing yield criterion of the plastic yield surface of the structure and is

determined from the m-n characteristic relation for a rectangular section (see [6]).

Jones [6] and Olson, Nurick and Fagnan [8] present predictions for the initiation of mode II failure (tearing) based on a maximum strain to failure concept. Both methods include bending and membrane strain. Neither considers the effects of shear on the result.

Jones' procedure uses the predicted deformation as discussed above and a prediction of strain based on the deformation.

$$\epsilon_f = 2\{(\frac{\delta_f}{t})^2 + \frac{L}{2t} - 1\}(\frac{t}{L})^2$$ [6:eqn. 7.140]

The impulse to rupture is predicted as that required to causes strain that is greater or equal to the rupture stain of the material. Thus:-

$$I = \{6\rho\sigma_o L^2 t^4 [\ \{1 + \sqrt{\frac{\epsilon_f}{2}(\frac{L}{t})^2 + 1 - \frac{L}{2t}}\ \}^2 - 1]\ \}^{1/2}$$

A similar method is used by Olson,Nurick and Fagnan [8] to predict mode II failure as part of a numerical solution.

The method also includes only bending and membrane strain, but differs in how the strains are calculated.

The bending strain is expressed as

$$\epsilon_b = \frac{t\kappa}{2}$$

where κ is the curvature and is defined as

$$\kappa = \frac{\frac{\partial \delta}{\partial \omega}}{l}$$

The membrane strain is approximated by

$$\epsilon_a = \frac{1}{2L}\int_0^L (\frac{\partial \delta}{\partial x})^2 dx$$

where δ is the shape of the deflected plate.

Teeling-Smith and Nurick [2] found that the shape of the deflected plate can be approximated by

$$\delta = \delta_f \, Sin \frac{\pi}{L} x$$

This is applied to the preceding equations to predict strain. The impulse is found from the predicted strain in the same way as in Jones' method.

The two methods predict similar membrane strain but differ in the calculation of the bending strain.

3.2. Experimental Work

Nurick and Martin [1] give an overview of the experimental work.

3.2.1. The Relationship Between Impulse and Deflection

data points was 109.

They also reported a relationship of:

$$(\frac{\delta}{t})_q = 0{,}471\phi_q + 0{,}001$$

for quadrangular plates, with a correlation coefficient of 0.984, where the number of data points was 156.

3.2.2. Impulse to Rupture

a) Circular Plates

Teeling-Smith and Nurick [2] determined a threshold impulse of 27.9 Ns (ϕ = 47) at a deflection of 18.2 thicknesses.

Nurick [10] observed tearing at an impulse of 15.6 Ns (ϕ = 25.5) at a deflection of 12.4 thicknesses. That result is presented here, but is not reliable as a comparison since no failure strain for the material was given and only one torn plate was observed in a series of experiments.

b) Square Plates

Nurick [10] observed tearing at an impulse of 19 Ns ($\phi \approx 27$) at a deflection of 13.3 thicknesses, and again, no failure strain for the material was given and it was the only torn specimen in a series of experiments. Nurick and Shave [11] determined a threshold impulse of 10,8 Ns ($\phi = 17.4$) at 8 deflection thicknesses.

3.2.3. Necking

a) Necking in Circular Plates

In addition to the radial slip observed in previous experiments, necking has been recognized at the plate boundary by Nurick and Teeling-Smith [3] in circular plates. Nurick and Teeling-Smith do not make the distinction between radial slip and necking, but in ref.[2] they only recognize radial slip where the impulse is higher (I = 30 N.s. compared with I = 13 N.s.). The effect of necking is clearly shown as an increase in slope of the deflection-thickness versus damage number graph (fig.3.1) at a deflection of 10 plate thicknesses. This reflects a decrease in stiffness. The increase in slope was found to be 26%. There were 78 data points.

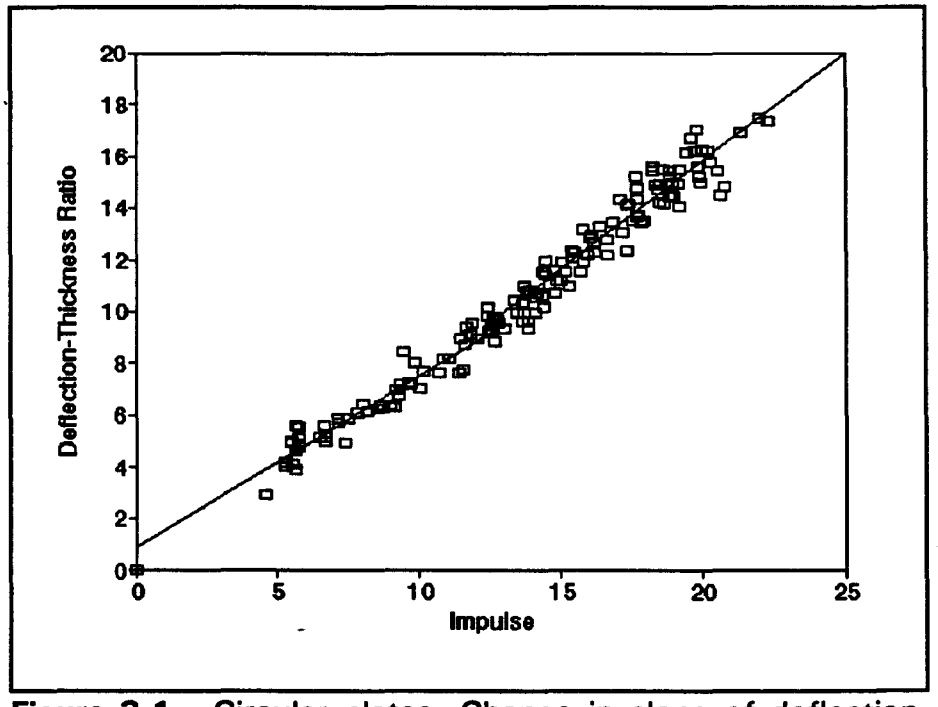

Figure 3.1 - Circular plates. Change in slope of deflection-thickness versus impulse graph, demonstrating the necking point. Ref[3].

As noted by Shen and Jones [5] in section 3.1.1 a decrease in stiffness can be attributed to a lack of radial constraint. Thus, necking may indicate radial slip.

The necking point indicates the initiation of necking, with possible associated slip, and decreasing stiffness at a deflection of about 10 plate thicknesses, at a damage number of approximately 23 (or I ≈ 13 N.s.).

This necking point can be used to define two different types of Mode I failure: Mode I(a) - Mode I failure with no necking, and Mode I(b) - Mode I failure with necking.

b) Necking in Square Plates

The results of Nurick [10] for square plates shows similar behaviour at a cutoff deflection of around 9 plate thicknesses (fig.3.2). This has not been reported before, but is analogous to the work done on circular plates by Nurick and Teeling-Smith [3] described above. The value of 9 was arrived at by inspection of the graph of deflection versus damage number. Regression analysis of the data above and below the cutoff shows an increase in slope of 21% for the 39 data points. This is a persuasive argument to reach the same conclusions as Nurick and Teeling-Smith, that necking or thinning of the plate near the boundary occurs when the mid-point deflection, (and thus total strain,) is above a certain value. The impulse at which this occurs is approximately 13 N.s.

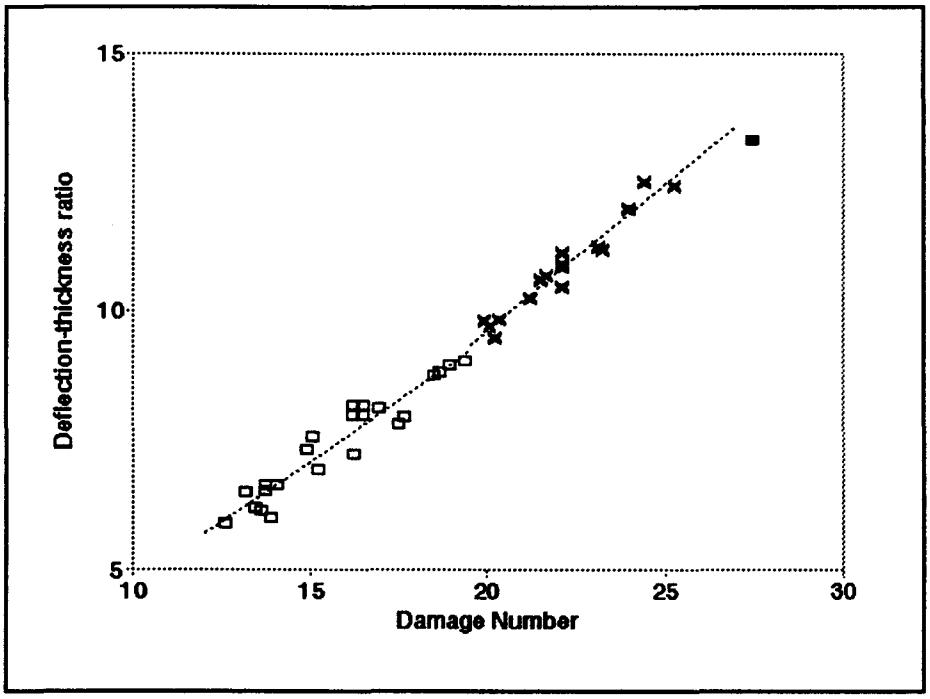

Figure 3.2 - Square Plates. Evidence of a necking point in the results of Nurick [10].

These cutoff values can be related empirically by the ratio of the aspect ratios, defined as:-

$$\frac{\frac{R}{t}}{\frac{L}{2t}} = \frac{10}{8.9} \approx \frac{10}{9}$$

To investigate this phenomenon closer a number of the specimens from Nurick [10], representing a range of deflection values were selected. These specimens were cut across their section and polished to reveal detail of necking at the boundary.

The photographs of the polished sections shown in fig.3.3 show closeups of the plate boundaries. It is difficult to identify the onset of thinning, but necking is clear

in the plates with large deformations and not visible in plates deformed less than about 8 thicknesses.

Figure 3.3 - Photograph of polished section of clamped square plates.(test no. 2404851, 0805856, 2504852, 0605854, 0605852, 1704854) Ref[10].

When viewed from the unloaded side of the plates (fig.3.4) a scraped area can be seen along the edges of the more deformed plates, probably caused by the surface of the plate being forced over the edge of the base plate. This could indicate a small amount of radial displacement associated with necking.

As the plate at the edges of the clamping plates thin, the plate becomes less constrained as the clamps do not close in with the thinning and the effect is that the plate is less restrained in the radial direction. This effect is best illustrated in a diagram in fig.3.5.

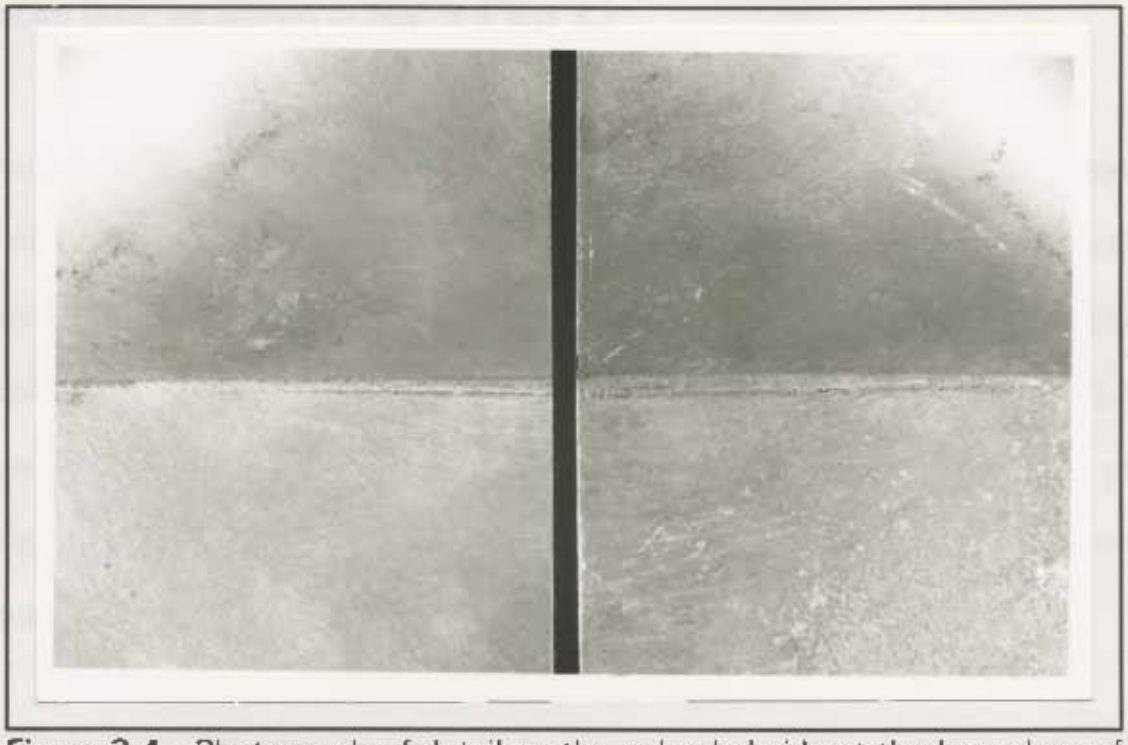

Figure 3.4 - Photograph of detail on the unloaded side at the boundary of clamped square plates. (Test no. 2404851 and 0605856)

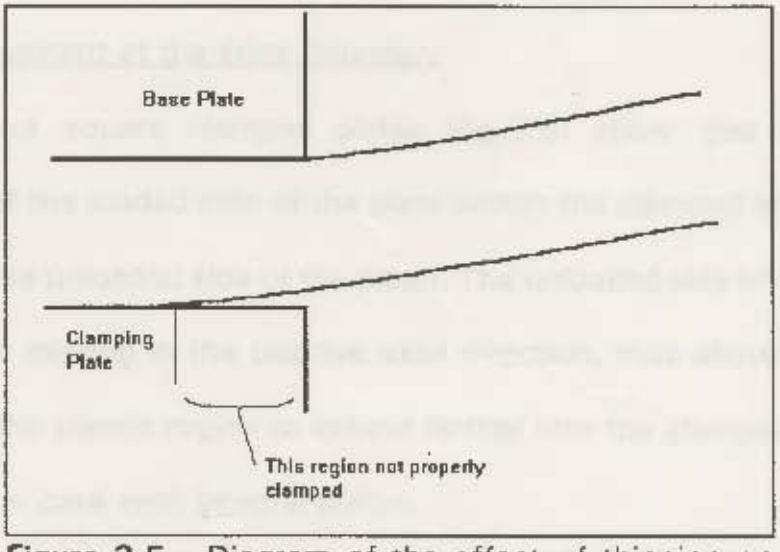

Figure 3.5 - Diagram of the effect of thinning on clamping.

According to Shen and Jones' argument presented in section 3.1.1 plates less constrained in the radial direction would be less stiff and should show a steeper deflection verses impact relationship. This is indeed the case at impulses above the

necking point as shown in figs. 3.1 and 3.2 .

To summarise the mechanisms of necking: At some point, called the necking point, thinning occurs at the plate boundary. This point can not be determined accurately by inspection of the plates, but can be identified as the point at which the plates becomes less stiff. Once the plate has thinned it becomes less tightly clamped, and allows movement in the radial direction. The radial movement results in the plate being less stiff and mid-point deflections higher than predicted are observed at impulses above the necking point.

These effects should appear only in mode I(b) failure modes, and should have no effect in the mode I(a) failure mode.

c) Axial Displacement at the Edge Boundary

Closeups of cut square clamped plates (fig.3.6) show that there is axial displacement of the loaded side of the plate within the clamped area (marked by a shear lift on the unloaded side of the plate). The unloaded side of the plate is not restrained from moving in the positive axial direction, thus allowing thinning to occur and for the plastic region to extend farther into the clamped region of the plate than in the case with integral plates.

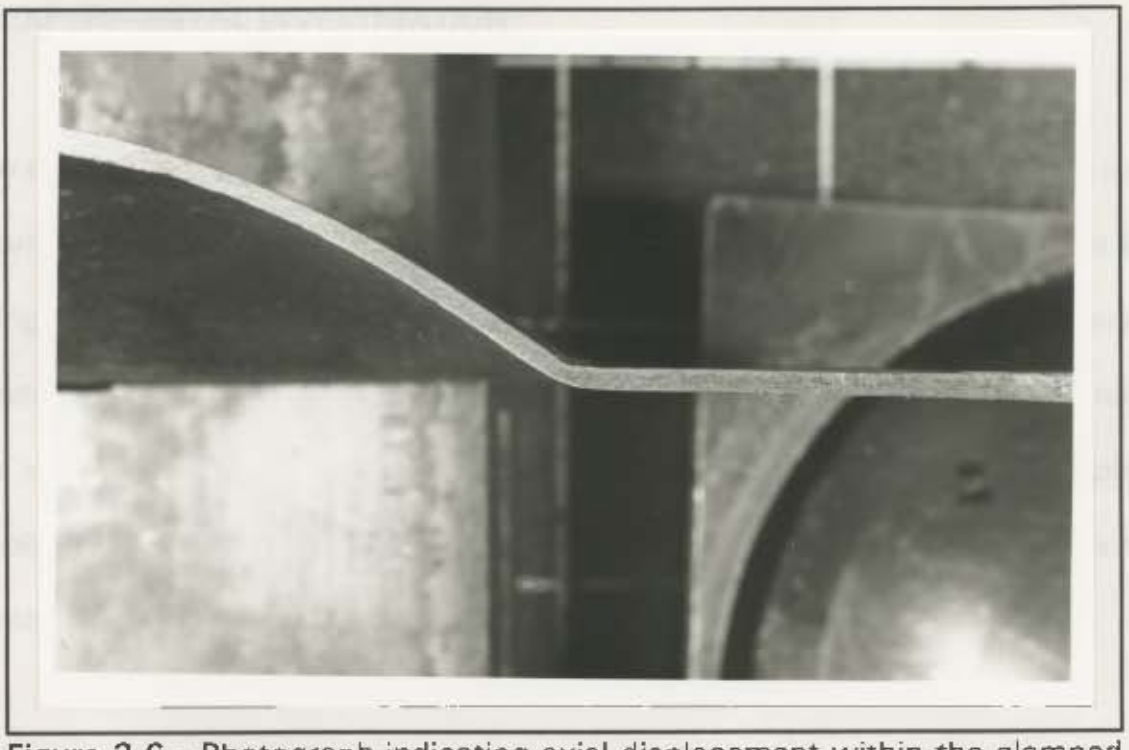

Figure 3.6 - Photograph indicating axial displacement within the clamped region of clamped plates. (Test no. 2404851)

4. EXPERIMENTAL INVESTIGATION

The experimental method used and presented here is similar to that used in many previous experimental investigations. The method of creating an impulsive load using plastic explosive and the measurement of the impulse using a ballistic pendulum is the same as used in previous experiments. The ballistic pendulum is the same as that used by Nurick et al [1,2,3,10,11] and several other projects involving explosive impact on plates. The experimental method used is thus well established and accepted.

The difference in these experiments is in the method of securing the plate. The aim of these experiments is to investigate the effects of different edge boundary conditions. This is examined by employing integral plates whereas previous experiments used a method whereby the plates were clamped.

This chapter describes the experimental investigation. Firstly the data required is listed, then the equipment is described and the calculation needed to convert the results to the form required is given. The details of the plates and their difference from previous test specimens are described. Lastly the experimental procedure is described.

4.1. Required Data

The data required for analysis is :-

1. The impulse on each plate.
2. The dimensions of each plate.
3. The properties of the material used for the plates.
4. The mid-point deflection of each plate.

4.2. Experimental Equipment

The equipment used can be divided into three categories:-

1. The ballistic pendulum, used to measure the impulse.
2. The explosive, used to impart the impulse.
3. The test specimens.

4.2.1. The Ballistic Pendulum

A diagram of the ballistic pendulum is given in figure 4.1. The ballistic pendulum consists of an I-beam suspended from the ceiling of the 2,5m x 3,5m blasting room by four spring steel cables. These cables are adjustable to allow the pendulum to be levelled. The plate mounting assembly is attached to one end of the pendulum and a balancing arm and recording pen to the other.

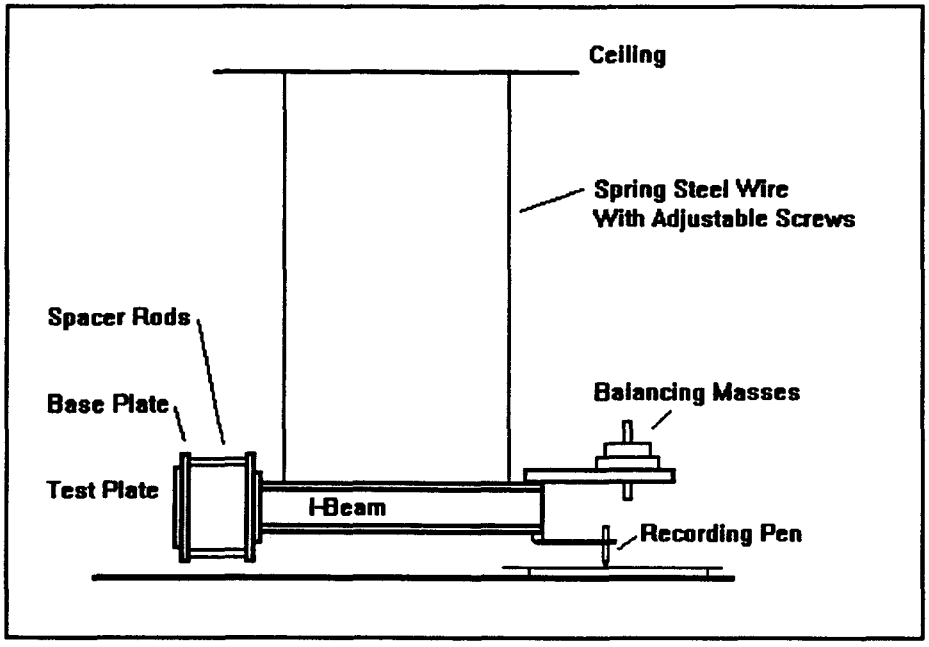

Figure 4.1 - Ballistic pendulum configuration.

The plate mounting assembly consists of a heavy steel plate which bolts onto the I-beam, four spacer rods and a heavy steel base plate with the appropriate cutout to which the test plate is bolted. For some of the experiments where larger impulses were used longer spacer rods were required to allow for a catcher box. The catcher box is a box filled with aluminium shavings used to catch plates which have blown out fully, without damaging the deformed piece.

At the other end of the pendulum is an arm on which balancing masses can be mounted. These balancing masses ensure that the pendulum is level, that suspending wires takes similar loads, and that the impulse acts through the centroid of the pendulum.

The pen attached to the pendulum records the oscillation of the pendulum on tracing paper. The momentum imparted to a test specimen by the impulse is

related directly to the amplitude of the initial swing and this can be found from the recorded trace.

In order to calculate the impulse from the trace several measurements need to be taken of the apparatus. These, together with the calculations and formula used to relate trace length to impulse are presented in Appendix A.

4.2.2. Explosive

PE4 plastic explosive was used.

The explosive was arranged in the same manner as used by Nurick [10]. The arrangement is shown in figures 4.2a and 4.2b. A two ring and cross leader configuration was used for circular plates and a two concentric square annuli and cross leaders configuration was used for square plates. The cross leaders were attached to a detonator by a main leader at the centre of the plate.

The explosive was placed on a 14mm thick polystyrene pad cut to the same dimensions as the plate. This was done to attenuate the shock transmitted to the plate, provide a uniform impulse and prevent spallation of the specimen.

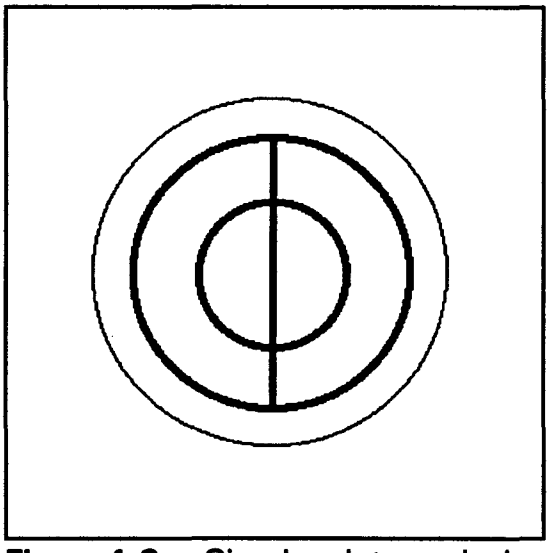

Figure 4.2a - Circular plate explosive layout.

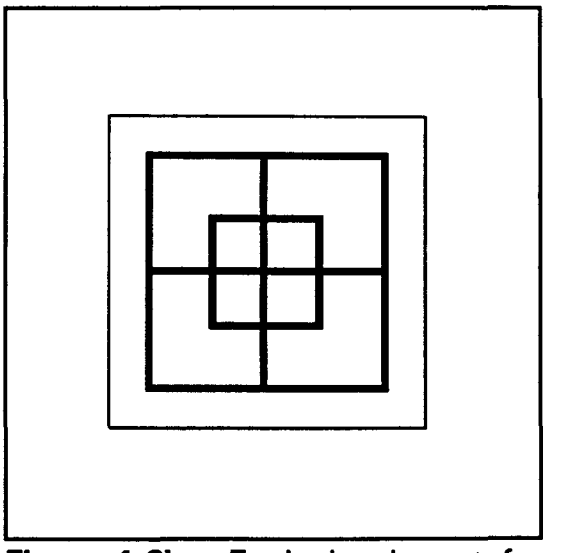

Figure 4.2b - Explosive layout for square plates.

4.2.3. Test Specimens

The test specimens used differ from those used in previous experiments. In experiments done previously, and whose results are used later for comparison, the equivalent specimens used were usually cut from 1.6mm cold rolled steel plate to a size of 200mm square or circular. The plates were then clamped between the base plate and a 20mm heavy steel plate with eight bolts. The base and clamping plate had the appropriate size and shape cut out. This arrangement is shown in figure 4.3.

The experiments described in this report do away with the clamping plate as shown in figure 4.4. The test specimens consist of 20mm thick approximately 200mm square plates with either a 89mm x 89mm square or 50mm radius disk machined out from either side of the plate, leaving a square or circular region of

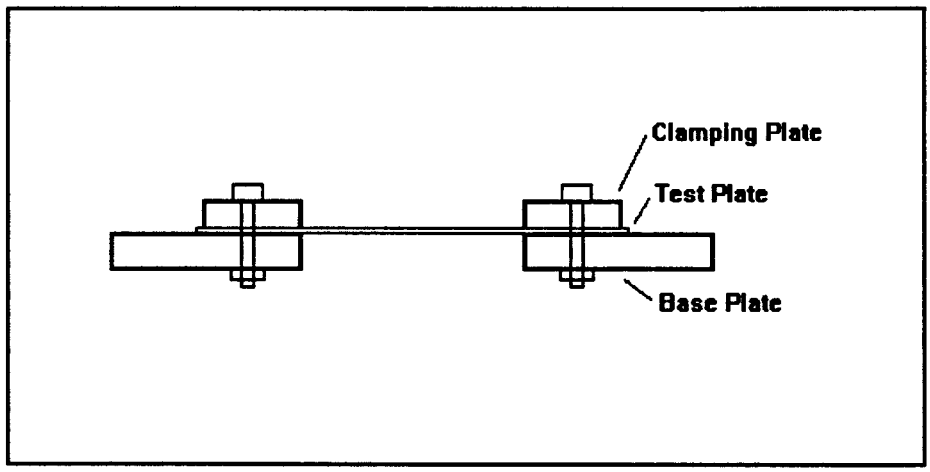

Figure 4.3 - Method used to clamp the plates in previous experiments.

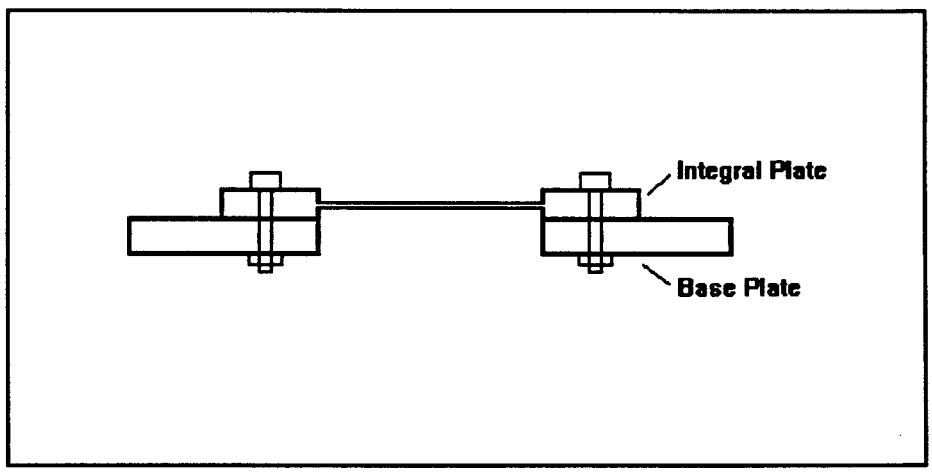

Figure 4.4 - Integral plate.

approximately 1,6mm thick steel near the middle of the plate. The blank plates were first smoothed off and roughed out on a lathe and then finished with a numerically controlled milling machine in order to ensure consistent dimensions and even thickness over the thin area. The plates were then heat treated to reduce possible machining stresses. The finished plate was measured and weighed.

In order to take into account the variable thickness of each plate, the thickness

was measured at several places on each plate. On the square plates the thickness was measured at 16 locations and on the circular plates at 13 locations (described in appendix B).

The plates were bolted directly onto the existing base plates.

Uniaxial tensile strength test specimens were cut from the thick parts of the test plates after testing and used to find the static yield strength and failure strain of the material. The static yield stress was determined using the results of uniaxial tensile tests at various quasi-static strain rates and substituted into the Cowper-Symonds rigid viscoplastic constitutive equation.

5. TEST RESULTS

A total of 47 tests are conducted, 17 on square plates and 30 on circular plates. 38 tests are preformed over a month and the remaining 9 three months later, thereby showing that good repeatability is possible.

Of the 30 tests completed on circular plates :-

- Two tore completely loose from the base. Both disks were too damaged from hitting the pendulum to take meaningful measurements of the mid-point deflections. In the case of the second plate (test 02069301) this happened despite the use of a catcher box.
- A total of 8 plates tore along part of their circumference. 5 of those tore along more than a quarter of the circumference and had lifted away from the plate by between 7 and 15mm at some point on the circumference. These tests were noticeably non-symmetrically deformed and were excluded from the results used to analyze deformation failure(mode I), only being considered in the analysis of mode II failure.

  They were tests:- 23039301

  23039304

  02039301

  02039305

  02069309

Of the 17 tests completed on square plates:-

- A total of 5 plates tore along their edges
- One plate tore along two edges and around the corner between them.(test 093931)
- One plate tore on two edges and not at the corner (test 0203933)
- Three plates tore along one edge only.

5.1. Test Readings

5.1.1. Plate Dimensions

The plates were weighed and the thickness measured. The thickness of each plate is determined as the average of the individual reading over the entire surface as presented in appendix B.

5.1.2. Impulse

The initial deflection of the pendulum is measured and the impulse is determined as described in appendix A.

5.1.3. Measured Deflection

The final mid-point deflection is measured using a depth micrometer and a ball

bearing to take into account the concavity of the surface of the plate.

5.1.4. Results of the Uniaxial Yield Tests

These are detailed in appendix C. The average value for static yield stress (σ_o) was found to be 262 MPa. The strain to failure (ϵ_f) was 40% . Both these values are used in later analysis.

5.2. Table of Test Data

Tables 5.1 and 5.2 list the test results for circular and square plates respectively. The data is listed under the headings; test number, explosive mass, plate thickness, impulse, damage number, mid-point deflection, deflection-thickness ratio, and type of failure.

The data is listed in order of increasing deflection-thickness ratio.

5.3. Experimental Observation

5.3.1. General Observations

In all the experiments where tearing did not occur, failure conforms to the Mode I category of large inelastic deformation. Of some importance here was the profile of the deformed section, and detail of the section at the boundary.

Test No.	Explosive Mass (g)	Thickness t (mm)	Impulse I (N.s.)	Damage No. ϕ	Mid-point Deflection d (mm)	d/t	Mode of failure
23039310	7.6	1.739	4.64	6.80	5.63	3.237	I
23039306	7	1.972	5.84	6.66	6.51	3.301	I
23039309	7.3	1.769	5.85	8.29	7.65	4.324	I
23039308	7	1.695	6.02	9.31	8.25	4.868	I
23039307	7	1.583	5.68	10.06	7.8	4.927	I
22039301	7	1.658	6.76	10.92	9.5	5.730	I
22039303	8.2	1.848	12.19	15.85	12.1	6.549	I
22039310	10	1.760	10.52	15.07	11.53	6.551	I
22039302	7.9	1.684	10.08	15.78	11.2	6.651	I
22039305	9.1	1.745	11.22	16.35	12.5	7.162	I
22039308	10.6	1.779	12.59	17.66	13.4	7.531	I
22039306	9.7	1.629	10.00	16.72	13.7	8.409	I
22039304	8.5	1.675	12.02	19.00	14.2	8.476	I
23039303	10.6	1.747	13.66	19.87	15.36	8.793	I
2069303	10.6	1.761	15.33	21.95	16.4	9.3141	I
23039302	10.45	1.713	14.19	21.46	15.96	9.317	I
2069302	10.3	1.717	14.10	21.23	16.92	9.8548	I
2069307	10.45	1.727	14.83	22.07	17.25	9.9889	I
22039311	10.45	1.769	16.64	23.59	17.68	9.993	II
23039305	10.45	1.696	17.33	26.74	19.45	11.47	II
2069308	9.7	1.582	14.59	25.86	19.04	12.033	I
2069309	10.6	1.748	18.74	27.24	22.58	12.92	II
22039307	10.3	1.629	17.85	29.85	21.25	13.04	II
2069304	10	1.541	16.30	30.48	20.96	13.604	I
23039304	10.45	1.645	18.21	29.85	23.54	14.31	II
2069305	10.45	1.627	17.52	29.39	23.28	14.309	II
23039301	10	1.575	15.75	28.19	23.66	15.03	II
2069306	10	1.595	18.75	32.74	24.33	15.258	II
22039309	10.9	1.544	18.20	33.90	*	*	III
2069301	11.2	1.597	19.48	33.92	*	*	III

Table 5.1 - Results of the tests done on circular plates.

Test No.	Explosive Mass (g)	Thickness t (mm)	Impulse I (N.s)	Damage No. ϕ	Mid-Point Deflection d (mm)	d/t	Mode of failure
203931	7.3	1.660	6.64	9.44	8.47	5.102	I
803935	7.6	1.646	7.25	10.47	9.04	5.491	I
803934	8.5	1.651	7.43	10.68	9.51	5.761	I
803938	10	1.588	8.10	12.59	10.33	6.505	I
903932	9.4	1.591	8.28	12.82	10.48	6.586	I
803933	9.4	1.600	8.98	13.74	10.56	6.6	I
803932	10.3	1.550	9.49	15.48	11.29	7.284	I
803931	10.3	1.602	8.28	12.64	11.68	7.291	I
903933	9.4	1.519	8.45	14.35	11.24	7.398	I
203933	10.3	1.641	12.37	17.98	13.35	8.134	II
903935	9.4	1.399	8.80	17.62	11.78	8.422	I
203932	8.8	1.450	8.11	15.11	12.57	8.669	I
803939	10.3	1.659	12.80	18.22	14.61	8.808	I
803936	10.6	1.620	12.46	18.60	15.08	9.309	II
803937	10.45	1.626	14.91	22.11	17.2	10.58	II
903934	9.7	1.466	11.58	21.10	16.22	11.06	II
903931	10	1.621	13.34	19.88	*	*	II

Table 5.2 - Results of the tests done on square plates.

Photographs of deformed circular and square plates cut across their section are shown in figures 5.1a and 5.1b respectively.

The following may be noted on the photographs:-

- Necking is not noticeable on any of the square plates.
- On the circular plates where there does appear to be necking (fig. 5.2 of tests 2069307 and 23039302), there is no evidence of radial slip of the back of the plate. These plates were near the threshold of mode II failure suggesting a small region of mode I(b) failure.

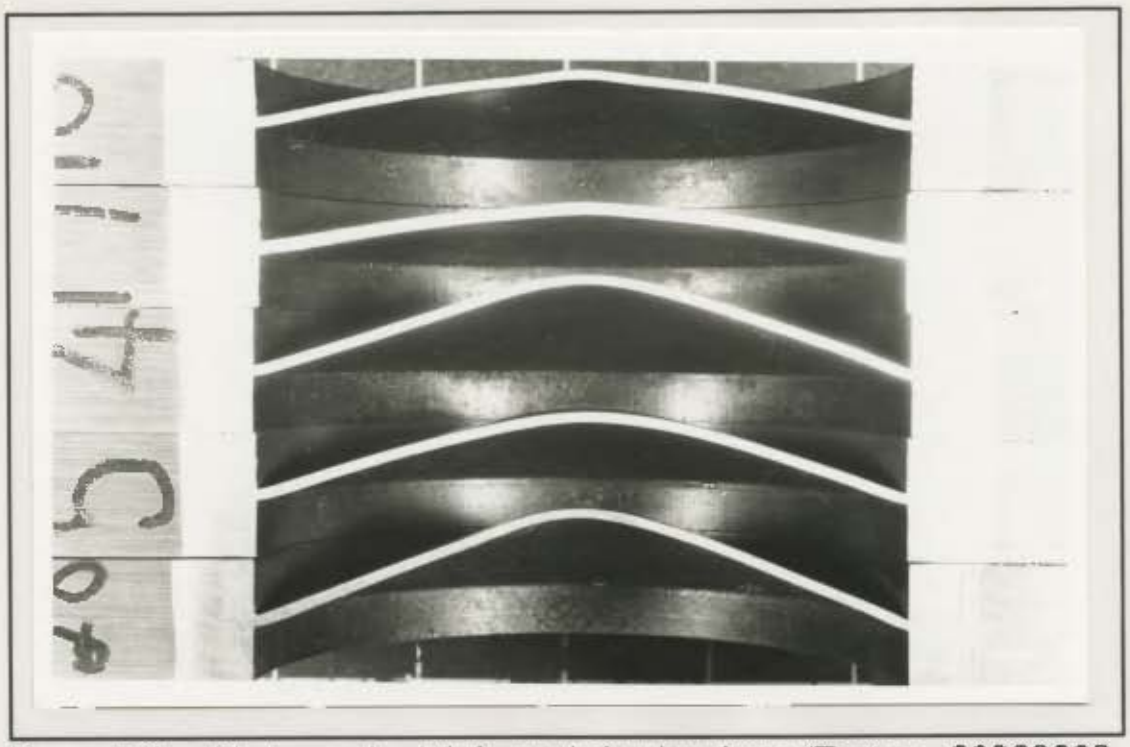

Figure 5.1a - Photograph of deformed circular plates.(Test no. 23039308, 23039306, 22039304, 22039305, 2069307)

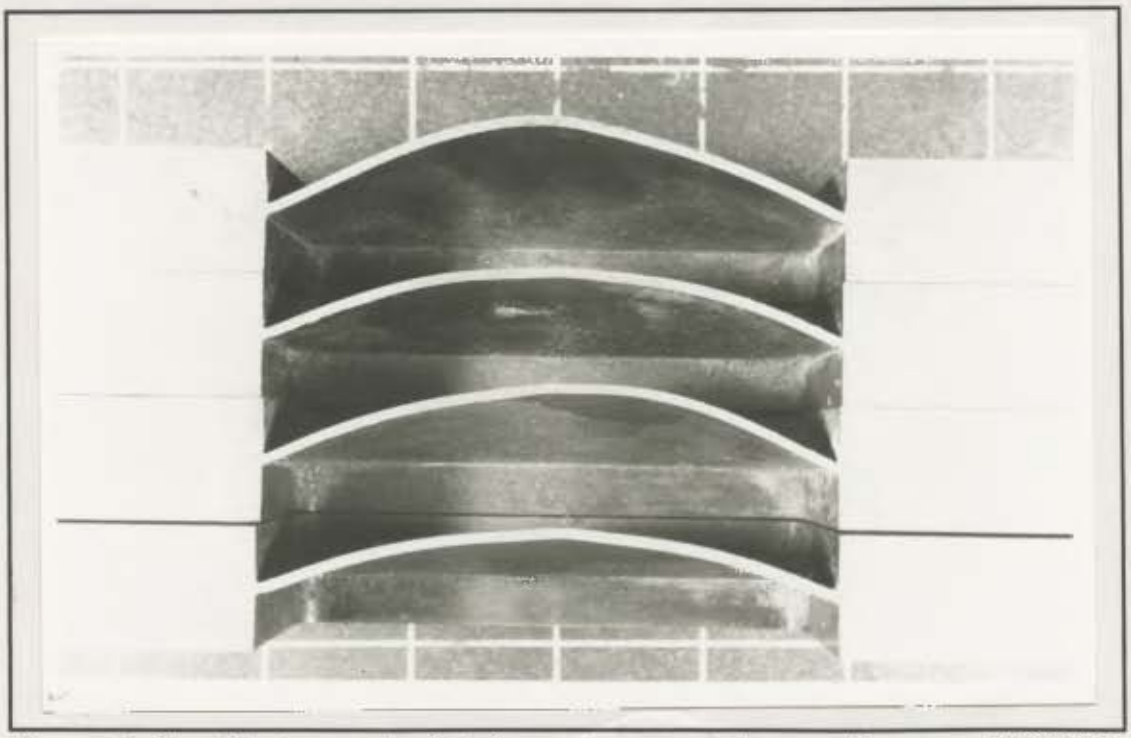

Figure 5.1b - Photograph of deformed square plates. (Test no. 803939, 803932, 803932, 803935)

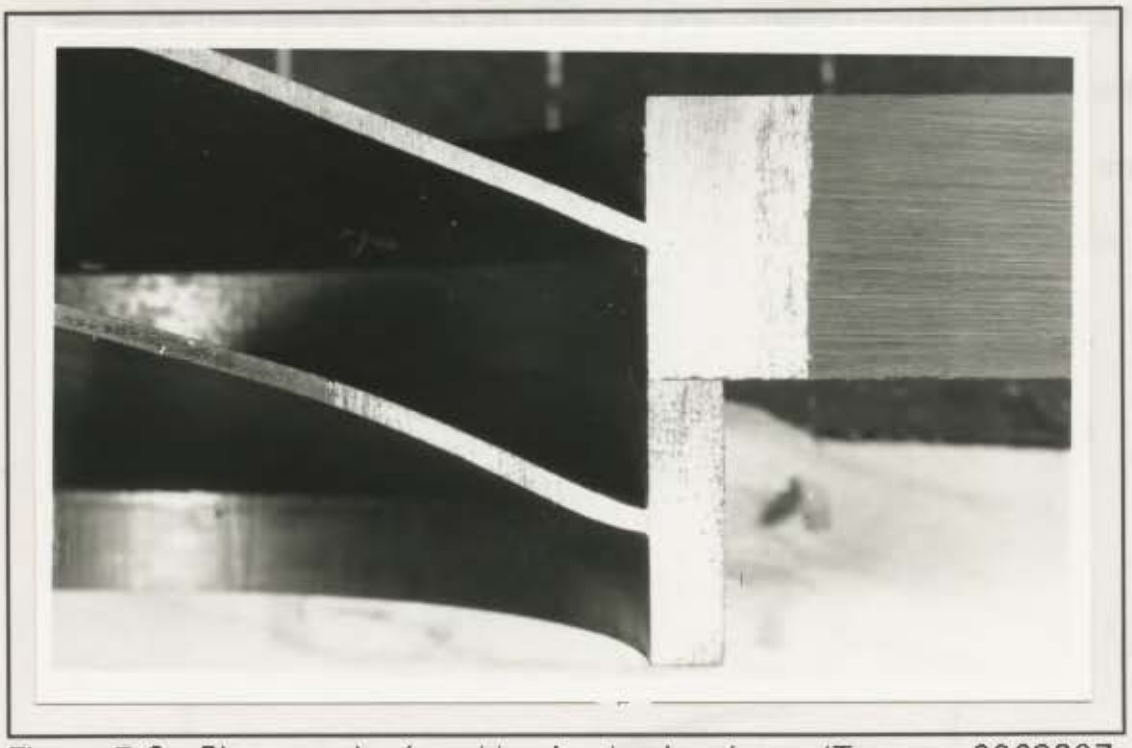

Figure 5.2 - Photograph of necking in circular plates. (Test no. 2069307, 23039302)

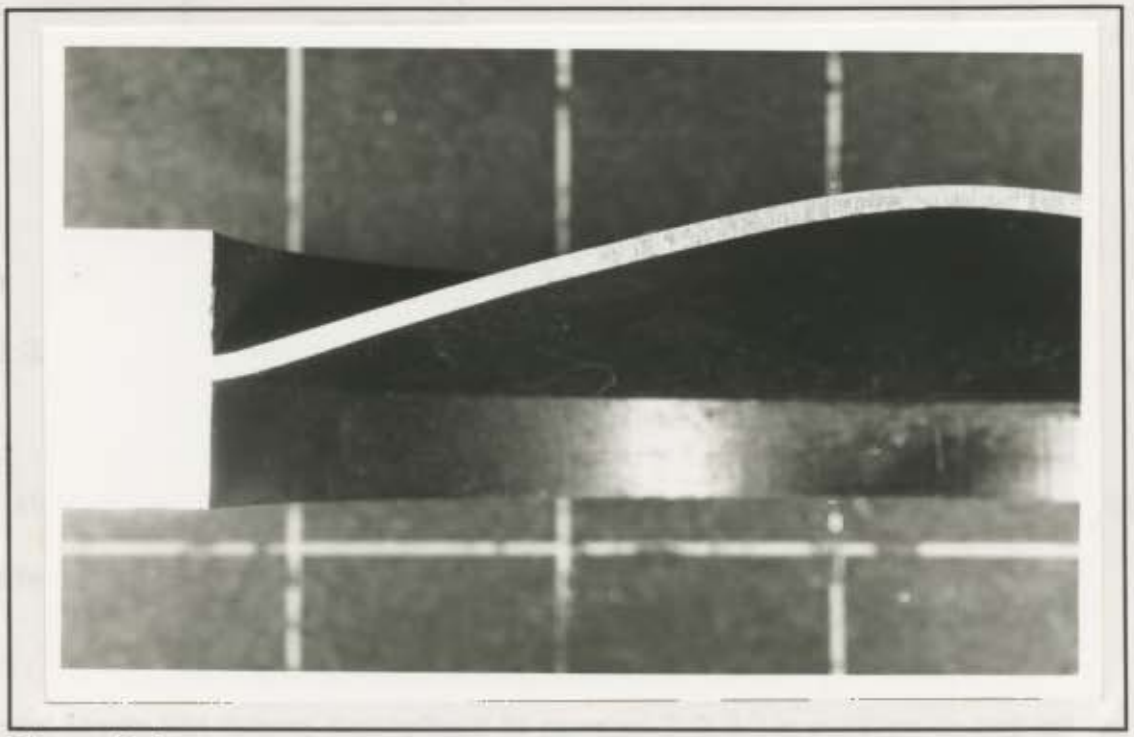

Figure 5.3 - Photograph of deformed profile near the boundary.(Test no. 22039305)

- On all the plates the curvature near the boundary was opposite to that at the

centre of the plate (eg. fig.5.3). This is a phenomenon apparent in numerical solutions [6], but not observed in previous experiments. This effect described more clearly in figure 5.4. The curve of the integral plate starts at the edge, whereas the curve of the clamped plate starts within the clamped region.

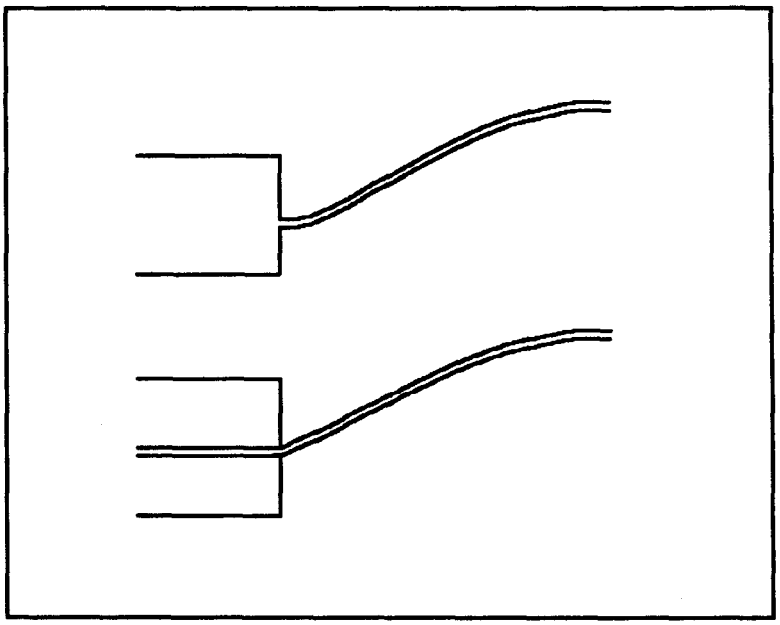

Figure 5.4 - Diagram showing the difference of curvature near the boundary between integral and clamped plates.

5.3.2. Type of Failure

As stated above, all tests where tearing did not occur can be considered to be Mode I failure - large inelastic deformation.

Partial Mode I(b) failure (as defined in section 3.2.3.) is evident in two of the 9 circular plates cut, where there is some thinning, but no radial slip. This occurs at an impulse above the necking point found by Nurick et al [3] and close to causing

rupture and is therefore confined to a small range of impulse. The untorn circular plates below the necking point and all the square plates can be considered to have failed in mode I(b).

The mode of failure of the torn plates is not as easy to identify and does not conform to either mode II or mode III failure as previously defined. Of the circular plates the clearest example of this is shown in figure 5.5 of test no. 22039307. There is clear shear failure along a surface about 45 degrees to the surface of the plate, and not enough necking to suggest tensile tearing, despite the impulse being only on the threshold of Mode II failure (not enough to cause complete tearing of the plate) and having a deflection-thickness ratio of 13. This can also be seen in test 23039305.

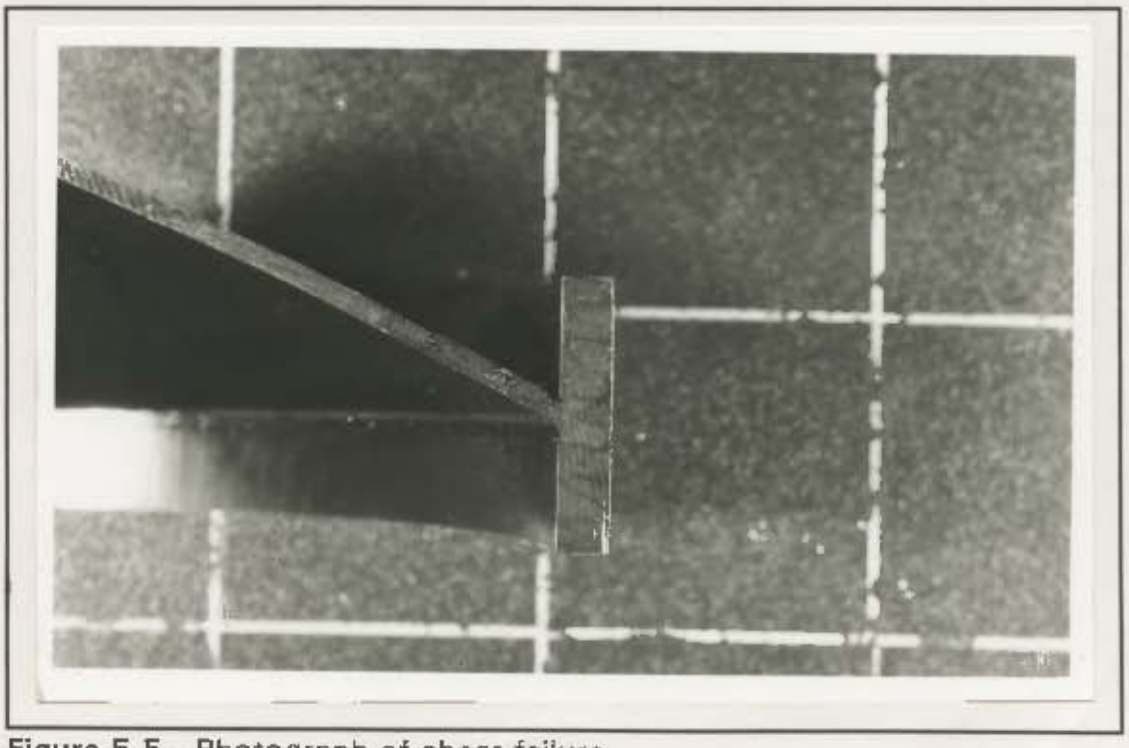

Figure 5.5 - Photograph of shear failure.

The cut square plates show similar evidence of shear failure, no necking and, more obviously than in the circular plates, evidence of progressive tearing beginning near the middle of a side and progressing towards the edges as described by Olson et al [8].

6. DISCUSSION

This chapter compares the results with existing theoretical and experimental work. Three aspects are compared:-

-The deflection verses impact relationship,

-The impulse to failure, and

-The type of failure exhibited.

The chapter closes with a discussion of the overall effects of the boundary condition used in these experiments.

6.1. The Relationship Between Impact and Deflection

This section looks at the relationship between impact and deflection mostly of Mode I failure, but in some cases the analysis can and does include tests where the plates have torn insufficiently to cause visible asymmetric distortion of the plate.

As has been stated earlier, the plates were not of consistent thickness. This resulted in the graph of deflection versus impact being more scattered than normally would be the case with experiments conducted in the past where the thickness of the specimen was more tightly controlled, having been cut from the same rolled sheets and clamped.

A procedure to resolve this problem is to use dimensionless numbers. In this case

the deflection-thickness ratio (δ/t) and the damage number (ϕ) are used instead of the deflection and impulse.

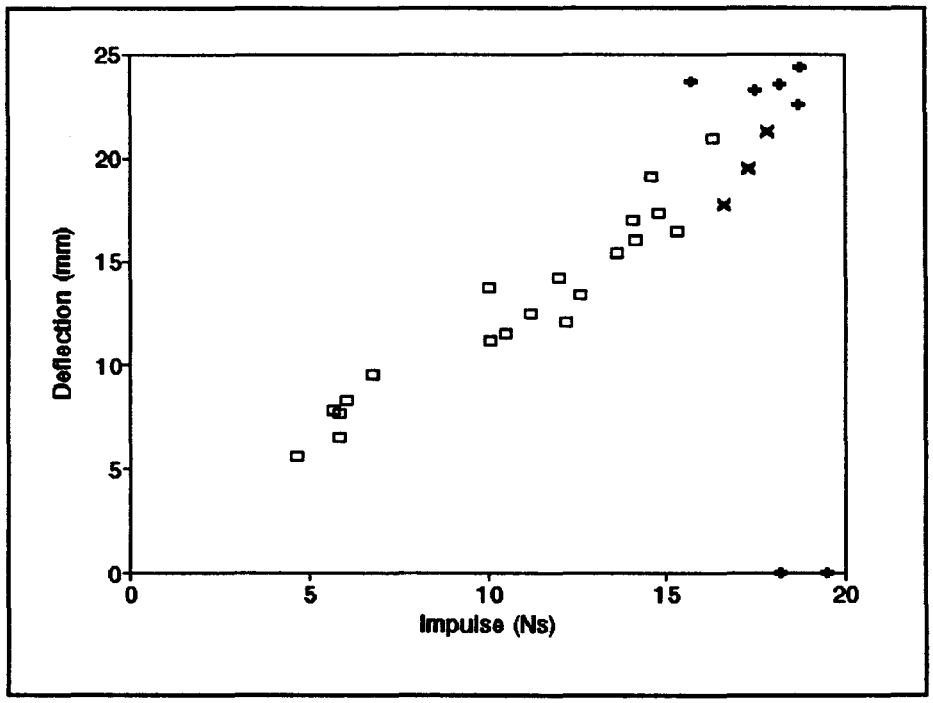

Figure 6.1 - Circular plates. Deflection versus impulse. □ - Plates that were measured, X - torn plates used in the calculations, + - torn plates not used in the calculations.

This method has been shown to be effective in comparing tests using specimens of different material properties, geometries and having different loading conditions [1]. A comparison of the graph of deflection versus impulse (fig. 6.1) with the graph of deflection thickness ratio versus damage number (fig. 6.2) reinforces the usefulness of the dimensionless number approach and highlights the effect of thickness on the plate response.

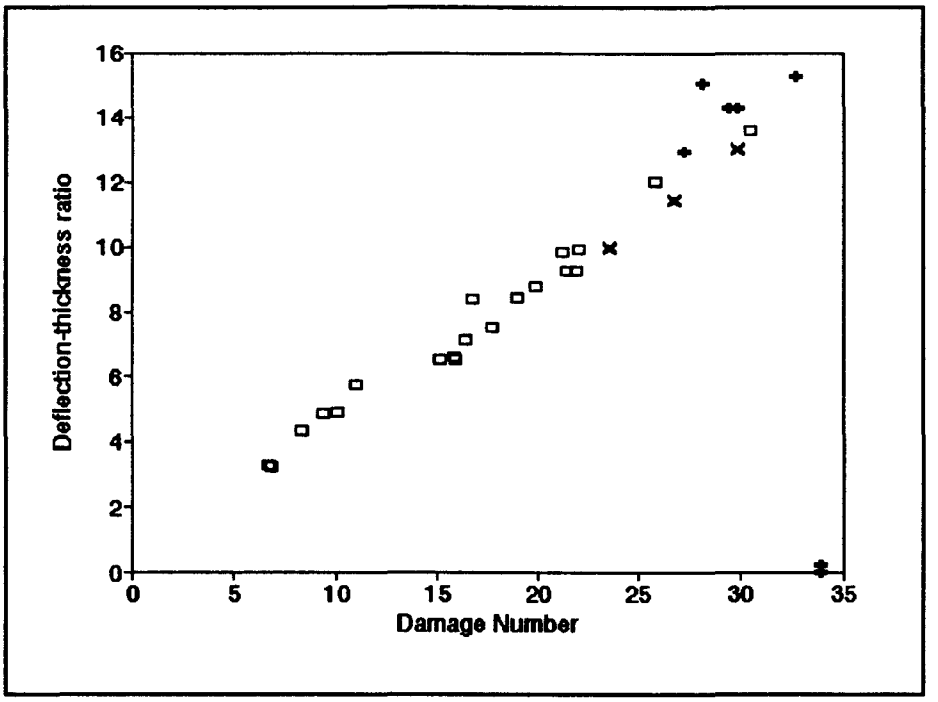

Figure 6.2 - Circular plates. Deflection-thickness ratio versus damage number.

6.1.1. Comparisons With Other Experimental Work

a) Circular Plates

The results of the tests done on circular plates are shown graphicly in fig. 6.2.

A least squares analysis was performed on the results. The analysis included all 20 untorn plates as well as three torn plates where the tear was insufficient to cause visible asymmetrical distortion of the plate.

The results of the least squares analysis is shown on fig. 6.3 with a ±1 deflection-thickness ratio confidence limit. The ±1 deflection-thickness ratio confidence limit was found by Nurick [10] to correspond closely to the 90% probability.

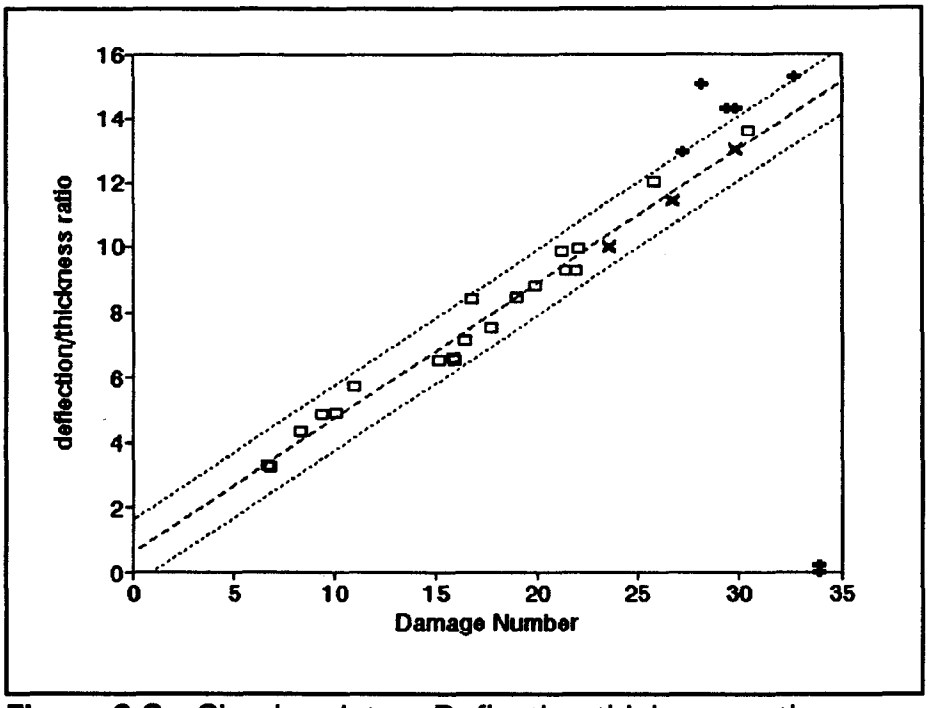

Figure 6.3 - Circular plates. Deflection-thickness ratio versus damage number with best fit line and ±1 confidence limit.

The analysis yielded a relationship of:

$$(\frac{\delta}{t})_c = 0{,}415\phi_c + 0{,}617$$

for circular plates, with a correlation coefficient of 0.981, where the number of data points was 23.

This compares favourably with Nurick and Martin's [1] reported relationship of:

$$(\frac{\delta}{t})_c = 0{,}425\phi_c + 0{,}277$$

for circular plates, with a correlation coefficient of 0.974, where the number of data points was 109.

A comparison of the results with those of Nurick and Teeling-Smith [3], which

includes the effect of necking are shown in figure 6.4. shows close agreement between the results for clamped plates and the integral plates investigated here.

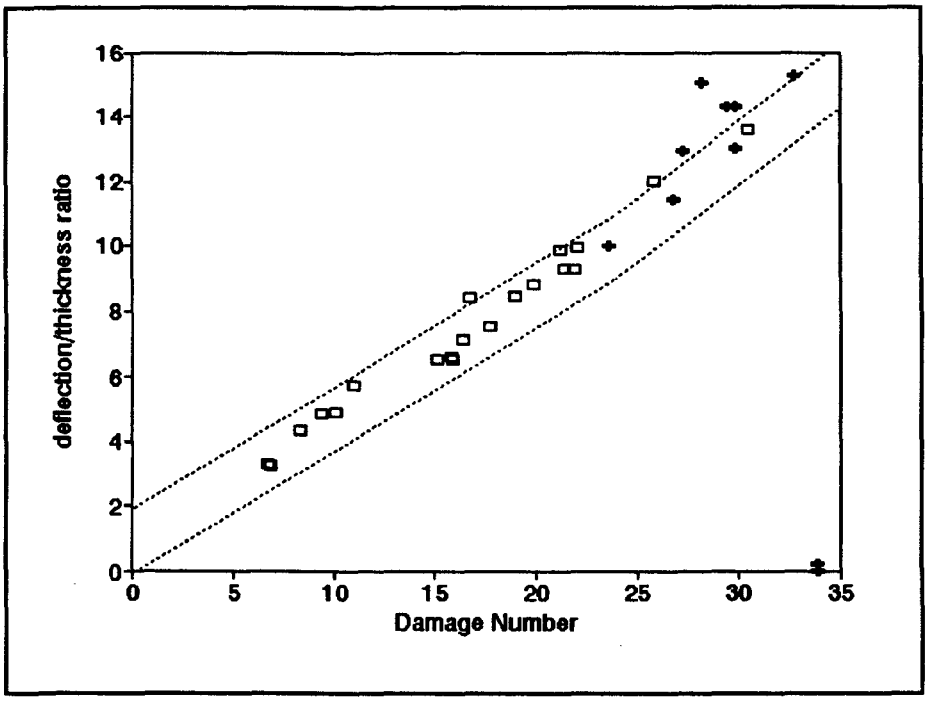

Figure 6.4 - Circular plates. A comparison of the results with the analysis of Nurick and Teeling-Smith [3].

a) Square Plates

The results of the tests done on square plates are shown graphically in fig. 6.5.

A least squares analysis was performed on the results. The analysis included all 12 untorn plates as well as four torn plates where the tear was insufficient to cause visible asymmetric distortion of the plate.

The results of the least squares analysis is shown on fig. 6.5 with a ± 1 deflection-thickness ratio confidence limit.

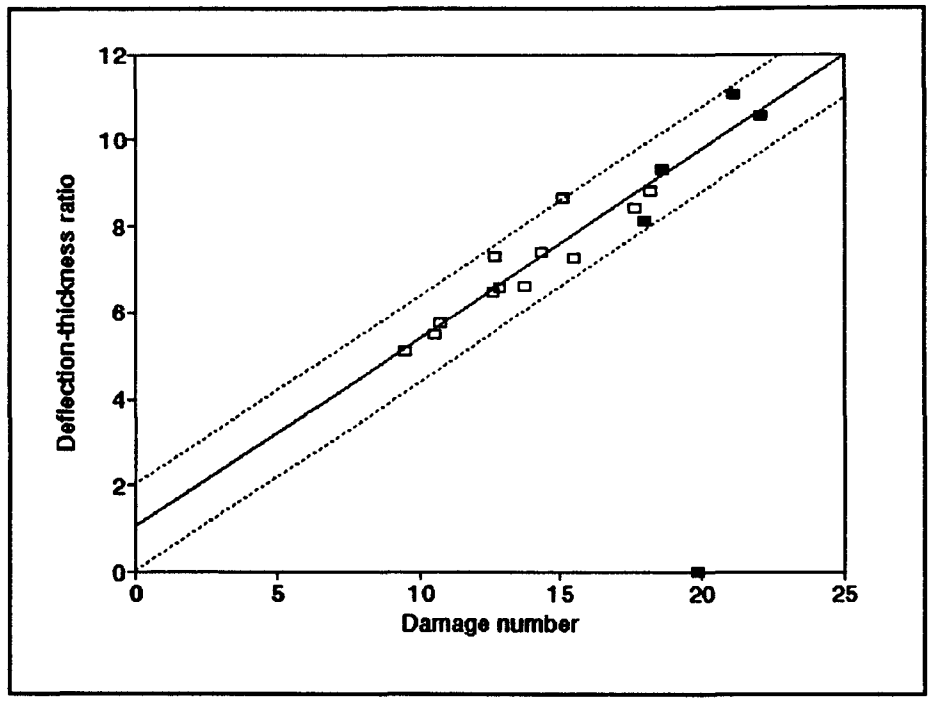

Figure 6.5 - Square plates. Deflection-thickness ratio versus damage number with best fit line and ±1 confidence limit.

The analysis yielded a relationship of:

$$(\frac{\delta}{t})_q = 0{,}438\phi_q + 1{,}033$$

for square plates, with a correlation coefficient of 0.922, where the number of data points was 16.

This compares well with Nurick and Martin's [1] reported relationship of:

$$(\frac{\delta}{t})_q = 0{,}471\phi_q + 0{,}001$$

for quadrangular plates, with a correlation coefficient of 0.984, where the number of data points was 156.

A comparison of the results with those which includes the effect of necking as found in section 3.2.3.(b) are shown in figure 6.6. Figure 6.6 shows close agreement between the results for clamped plates used in [10] and the integral plates investigated here.

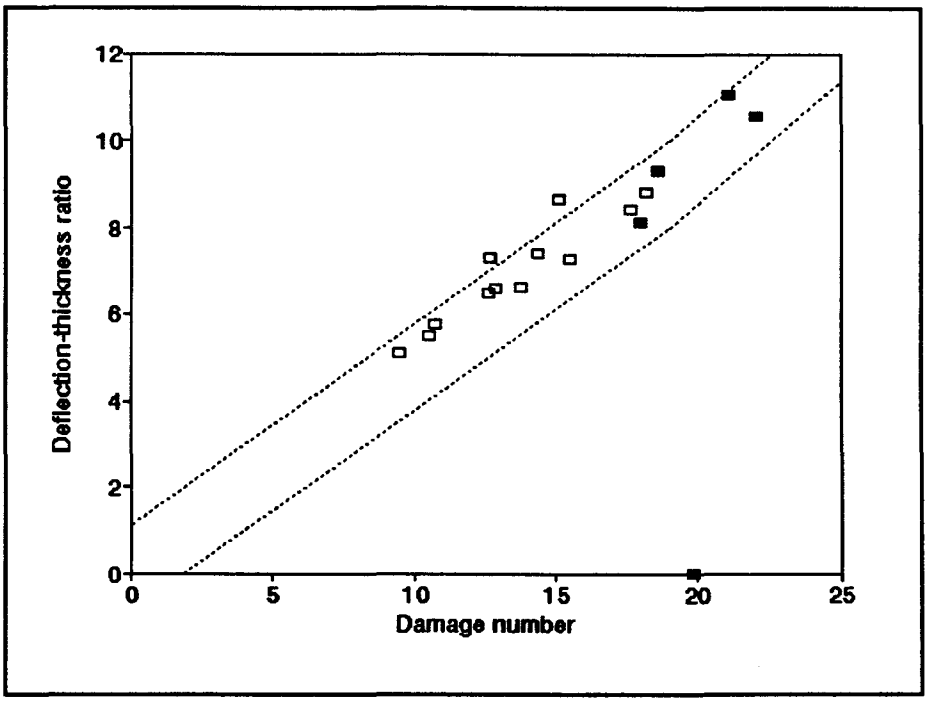

Figure 6.6 - Square plates. A comparison of the results with the analysis of section 3.2.3.(b).

6.1.2. Comparisons With Theoretical Work

a) Circular Plates

It is clear from figure 6.4 that the results from this investigation in which the plates are fully-built in are close to those achieved where the plates are clamped, for impulses resulting in mode I failure. Since the results are so similar, any comparison will not provide any new insights on the validity of theoretical solutions, other than that previous comparisons with clamped circular plates in the mode I range, are

valid. The reader is referred to reference [1] for a review of the theoretical solutions available.

A theoretical prediction by Shen and Jones [3] compares well for mode I with the experimental results of Teeling-Smith and Nurick [2]. It follows that this prediction is also valid for integral plates since integral plates display similar behaviour to clamped plates in mode I(a) failure range.

Jones' [6] method described in [7] predicts a deflection-thickness ratio as a function of the damage number and includes strain rate effects. Jones predicts:-

$$\frac{\delta_f}{t}=A\Phi$$

where **A**, which includes the strain rate effects, ranges is value from 0,583 at an impulse of 5 N.s. to 0,517 at an impulse of 15 N.s. Both these values are higher than the value of 0,415 yielded in the analysis of section 6.1.1.(a).

b) Square Plates

Less theoretical work has been done on square plates and fewer comparisons have been made. It is thus of value to include comparisons with theoretical predictions for square plates in order to asses the viability of extending the results of the circular plates to other geometries.

Jones [6] makes the prediction described in section 3.1.2.

Figure 6.7 shows the results for square plates with one line representing Jones' theoretical prediction not taking strain rate into account, and an upper and lower bound taking strain rate into effect.

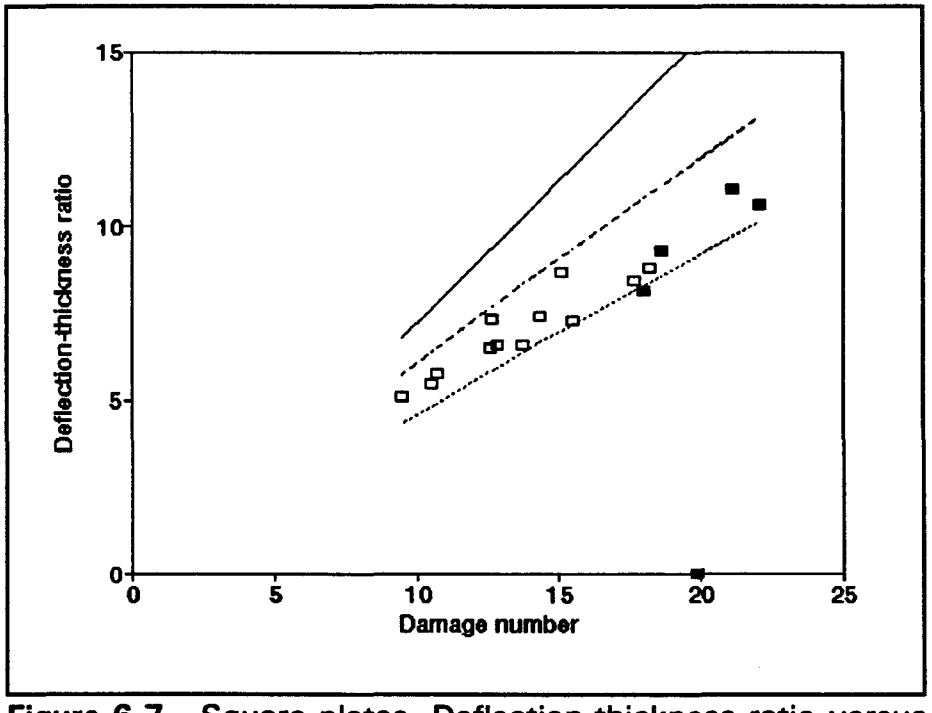

Figure 6.7 - Square plates. Deflection-thickness ratio versus damage number with Jones' prediction.—— without strain rate, --- upper bound, ... lower bound.

The results show good agreement with Jones' theoretical prediction. Fifteen of the 16 data points fall within the bounds. It is significant that the data points are *closely* bound by the theoretical upper and lower bounds. This suggests accurate assumptions of the mechanisms of failure of mode I failure.

6.2. Impulse To Rupture

6.2.1. Comparisons With Other Experiments

a) Circular Plates

The initiation of tearing does not occur at a fixed damage number or impulse due to the plates being of varying thickness. From a design standpoint it is more valuable to know the lowest impact to cause rupture or tearing. This is the threshold of mode II failure.

The results, as shown in figures 6.1 and 6.2, indicate a threshold of 15.75 Ns (test no. 23039301) or ϕ = 23,6 (no. 22039311) (defined in terms of impulse or damage number respectively). Note that these values were from different specimens, this is possibly due to the plates being different thicknesses. The threshold in terms of deflection/thickness ratio occurs at a deflection/thickness of approximately 10.

Several observations can be made about these results:

- The threshold values are significantly lower than those determined by Teeling-Smith and Nurick.
- Tearing occurs at a similar deflection/thickness ratio and damage number as necking in previous experiments.

A comparison of figures 6.1 and 6.2 shows a much smaller range between lowest

This is what is expected as it is used in the damage number. The boundary between mode I and II failure is more marked in figures 6.1 and 6.8 than in 6.9 (and 6.2). This suggests that the impulse to rupture is not best represented as being proportional to the inverse of the thickness squared. It follows that the damage number, ϕ, which is used to analyze deflection and is also proportional to the inverse of the thickness squared, is not valid for the prediction of mode II failure.

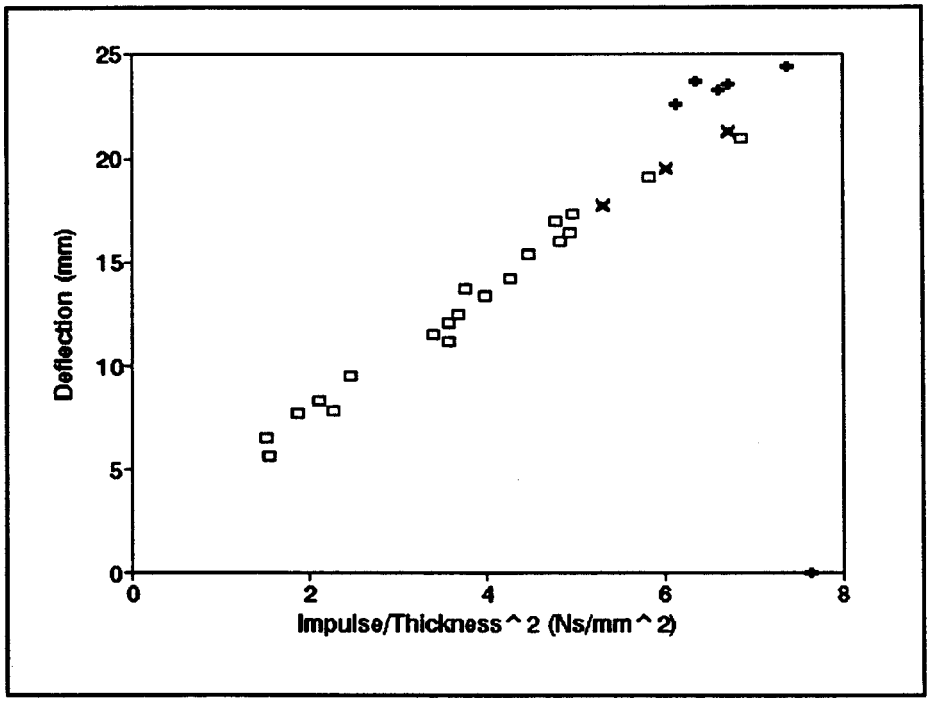

Figure 6.9 - Circular plates. Deflection versus impulse divided by thickness squared.

b) Square Plates

Tests were done on square plates only to check and extend on the work done on circular plates. Consequently there were fewer tests on square plates and fewer plates tore.

The threshold of mode II failure for the present square plates was 11.6 Ns in terms

of impulse (test no. 903934) or at a damage number of 18.0 (no.203933). The threshold in terms of deflection occurs at 8.1 thicknesses. As for circular plates, these were for different tests probably due to the influence of thickness.

These values are similar to those found by Nurick and Shave for clamped plates.

All the untorn plates have a deflection/thickness ratio less than the threshold of necking, as found in section 3.2.3(b). This is consistent with the observed absence of necking in the square plates.

6.2.3. Comparisons with Theoretical Work

a) Circular Plates

Shen and Jones [5] use a dimensionless number in their analysis which differs from that presented by Nurick and Martin [1] and used in comparing experimental results, namely I*, where :-

$$I^* = \frac{I}{\pi R^2 (\rho \sigma_o t^2)^{1/2}}$$

Using the analysis mentioned in section 3.1.1 a transition impulse of $I^* = 0.835$ was predicted using rupture strain value of $\epsilon_f = 1.376$ for a mild steel circular plate of the same dimensions. This value is used for comparison.

The results of the present tests are presented in a graph of deflection/thickness ratio vs I* in figure 6.10. Shen and Jones' prediction is represented as a vertical

line at I* = 0.835.

Figure 6.10 shows good correlation between the results and the theoretical prediction as a threshold value. No plates tore at a lower value of I* and only one remained untorn at a higher value.

Note, with reference to section 6.2.1(a), that I* is proportional to 1/t.

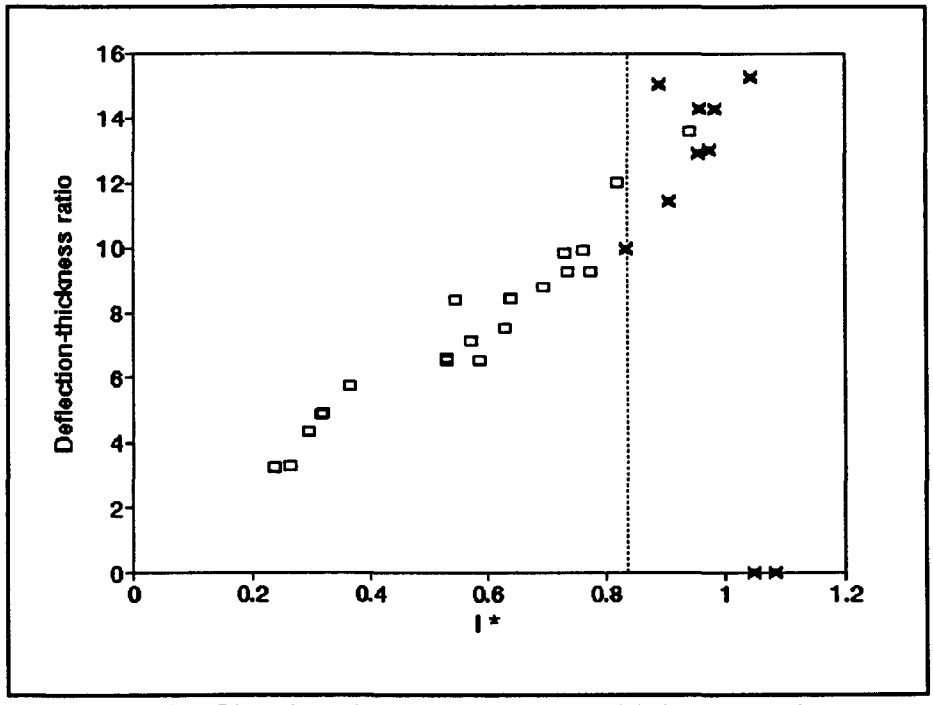

Figure 6.10 - Circular plates. Deflection-thickness ratio versus I*. Vertical line represents threshold predicted by Shen et al [3].

Jones'[6] prediction requires an iterative procedure. Assuming an impulse of 15 N.s. to calculate the strain rate factor n, yielded a damage number of 53 which translates to an impulse of 30 N.s. Although the solution to the equations can be improved by assuming an impulse of 30 N.s. to calculate n, it is clear from the

equations that the predicted mode II threshold will not improve, but increase.

It must be noted that Jones' solution uses bending and membrane strain does not include the effects of shear.

b) Square plates

Jones' theoretical prediction fails to give a value close to that recorded for the threshold of mode II failure in square plates.

Using Jones' method as suggested in [7], the threshold was found to be 20.3 N.s. with a corresponding damage number of 31.1. These are higher then the values found in this investigation of 11.6 N.s. and 18.

These values are further questioned when it is considered that the deflection from which the strain is calculated does not take strain rate into account. Section 6.1.2(b) and fig. 6.7 demonstrate the importance of taking the strain rate into account. Since it is the threshold that is required, it is appropriate to include the effects of the yield surface as well as the strain rate in the calculation of the deflection to be used in finding the strain.

The method used by Olson et al [8] produces results closer to those found in the experiments.

A useful way of presenting these approximations is to construct a graph of strain

versus impulse where the deflection is calculated from the impulse as per section 3.1.2 and the strain then calculated from the predicted deflection. This is shown in fig. 6.11.

The results of the calculations are represented as a line with theoretical prediction of failure at the impulse where the graph reaches the failure strain.

Figure 6.11 shows the strains predicted by the two methods discussed. The graph shows the strain predicted by the method used by Olson et al (0.25) to be far closer to the failure strain (0.41) than that found by Jones' method (0.1) at the threshold impulse of 12 N.s.

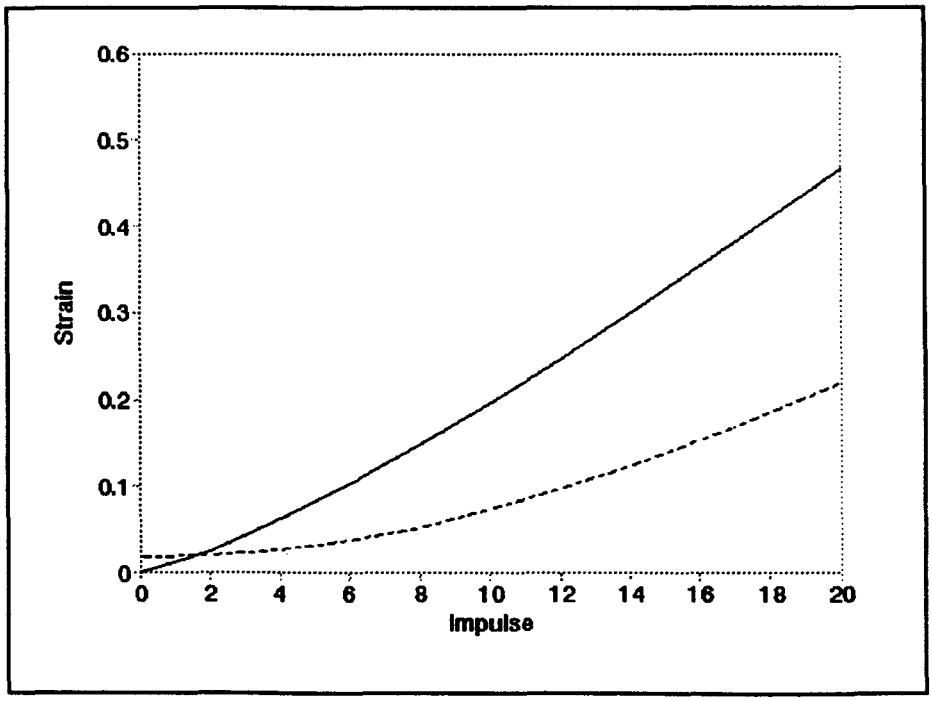

Figure 6.11 - Prediction of strain. ——— Olson et al [8] ; --- Jones [6].

Improvements notwithstanding, the predicted threshold impulse of 18 N.s , is still almost 50% higher than that found. This discrepancy can be attributed to a lack of understanding of the failure mechanisms and the consequent incorrect assumptions on which the theories are based.

It must be noted that neither of the predictions discussed above consider shear and both over estimate the impulse required for rupture.

6.3. Type of Failure

Mode I(a)

The majority of plates which showed mode I failure fell into the mode I(a) category. In the mode I(a) range the results were similar to those found in previous work utilising clamped plates. Consistent with the more symmetrical geometry, the deformation of the circular plates was more symmetrical, and perhaps for this reason these results were closer to those in previous work.

The only difference observed was in the shape of the deformed plate. With clamped plates, the maximum slope of the plate is at the edge, whereas these specimens displayed maximum slope a few thicknesses away from the boundary in agreement with numerical solutions. The curve of the bend at the boundary of the integral plates start at the boundary. The curve in clamped plates extend into the clamped region indicating a plastic region within the clamped part of the plate. This has no influence on the deflection in the mode I(a) range but becomes more

pronounced and has more influence at higher impulses.

Mode I(b)

The range of mode I(b) failure is small and only observed in circular plates.

This is consistent with the findings of section 3.2.3 which found the necking point for square and circular plates to be at 10 and 9 thicknesses respectively. Mode I(b) failure is expected when a plate remains untorn above the necking threshold. There are two untorn circular plates above 10 thicknesses and no untorn square plates above 9 thicknesses.

Necking

The necking point is found from the change of slope of the graph of deflection vs impulse as described in section 3.2.3. It is difficult to determine the necking point from inspection of the plates. Necking was not observed in the square plates, where all mode I failure was below the threshold of necking. Necking was observed in the more deformed of the circular plates, where some mode I failure was above the necking point. This does not disagree with the values found in section 3.2.3.

That tearing begins to occur at deflection-thickness ratios similar to those causing necking in clamped plates, suggests that through necking, clamping allows more freedom at the edge boundary and allows higher deflections without tearing.

Mode II

Previous reports [2] define Mode II failure as having a lower threshold taken as that impulse intensity which first causes tearing (tensile failure of outer fibre at the supports). Mode III failure is defined as being characterised by a well defined shear failure with no significant deformation in the severed central section.

The failure which has occurred does not conform to either category. There is clear shear failure along a surface about 45 degrees to the surface of certain plates despite the impulse being near the threshold of Mode II failure. This indicates the existence of significant shear in addition to the bending and membrane forces at work at the plate edge.

This supports the need to consider shear in any theoretical calculation of the impulse to cause mode II failure.

The sections of square plates show similar evidence of shear failure. Evidence of progressive tearing beginning near the middle of a side and progressing towards the edges as described by Olson et al [8] is also observed.

6.4. Discussion of the overall effects of the edge boundary conditions

This investigation examines the effect of edge boundary conditions on the failure of thin plates subjected to impulsive loading by comparing the results of tests

where different methods of securing the plates were employed. The results of work done previously using clamped plates are compared with tests using integral plates.

This discussion starts by summarising the similarities and differences observed between the results examined.

6.4.1. Summary of Similarities and Differences

Similarities

- When the dimensionless number ϕ is used, the deflection verses impulse relationship holds for both edge boundary conditions at impulses insufficient to cause necking .
- The general shape of the deformed plates are similar.
- Necking points appear to occur at similar deflection thickness ratios.
- The failure of square plates starting at the centre of the sides and propagating outward is common to both boundary conditions.

Differences

- The impulse and deflection to rupture was different for clamped and integral plates.
- The type of failure at the boundary. Clamped plates displayed necking and tensile tearing, the integral plates display less necking and more evidence of shear.

- The shape near the edge of the deformed integral plates is different to that of clamped plates. The plastic region extends beyond the boundary of the clamped plates.

6.4.2. Discussion of the differences

All the differences listed above occur at or near the edge of the plate and can be attributed to the differences in securing the plate. Clamping allows deformation within the clamped region of the plate allowing bending to occur beyond the plate boundary resulting in a different profile of the plate near the edge.

Clamping results in a less rigid boundary at impulses above the necking threshold. This allows more degrees of freedom at the plate boundary than is the case for integral plates. One of the results of this is to relieve shear strain which causes rupture to occur at higher impulses and to be in the form of tensile tearing.

6.4.3. Mechanisms at the Plate Edge

The type of boundary has an influence over the type of failure. In figure 6.12 an attempt has been made to show the difference in deformation at the boundary between clamped and integral plates. Most clearly, deformation of the plate occurs within the clamped portion of the clamped plate. Therefore, when modelling clamped plates, the plate edge - at the edge of the clamps - cannot be considered as the edge of the system.

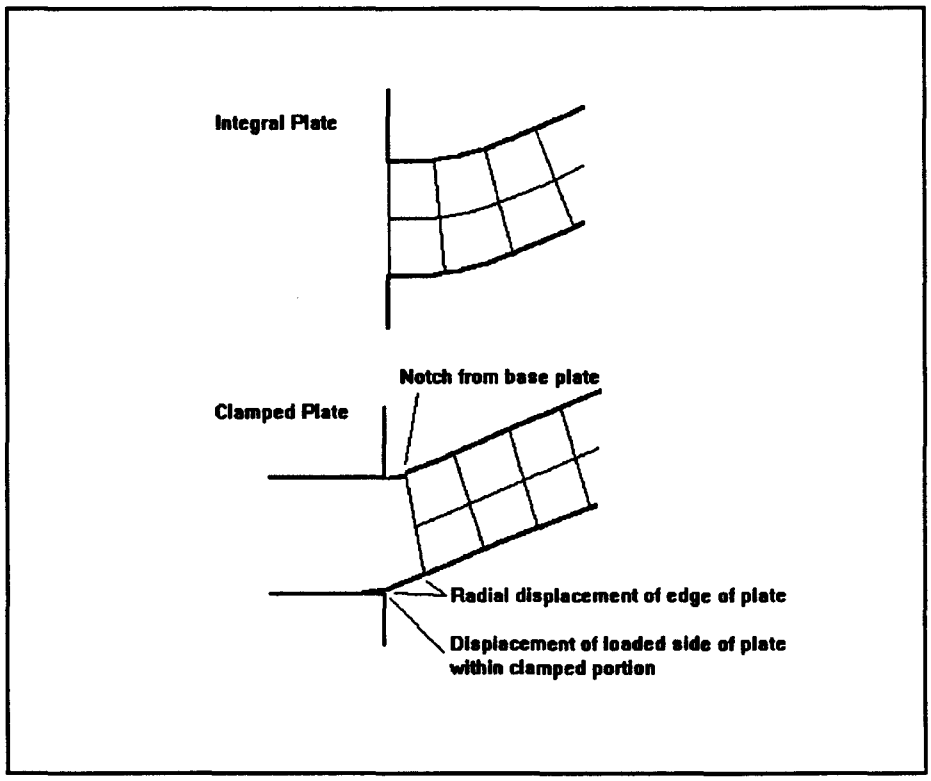

Figure 6.12 - Diagram of detail at the edge boundary.

An accurate prediction of rupture of clamped plates should model the clamping condition in more detail.

The predictions of Shen and Jones [5] for circular plates are more accurate when applied to integral plates due to the system boundary conforming more to the assumed - rigid - boundary at the plate edge.

The mechanism of rupture for integral plates appears to have a larger shear component than for clamped plates. Firstly, inspection of the deformed plates and analysis of the results of ruptured plates of different thicknesses suggest a shear component in mode II failure. Secondly, it is significant that the prediction of mode II failure by Shen and Jones [5] that includes shear is confirmed while those of

Jones [6] and those of Olson et al [8] that do not include shear are not confirmed.

7. CONCLUSIONS

The effects of the edge boundary conditions were investigated by comparing the results of experiments involving integral plates with previous experimental work using clamped plates. As a result of the investigation, the following conclusions can be drawn.

- Changing the plates from being clamped to being integral has negligible effect on mode I(a) failure. There were insufficient results in the mode I(b) range to conclude anything about the effect on mode I(b) failure. Mode II failure occurred at lower impulses for integral plates, and appeared to have a higher shear component in their failure.

- The results of previous experiments using clamps to secure the plates are valid for impulses below the necking point. The use of the damage number is successful in analyzing results for mode I where thickness varied, but not for determining the threshold of mode II failure. Empirical relations for mode I failure derived from previous experiments, such as those derived by Nurick and Martin [1] are valid. However these empirical relations may be improved by considering mode I(a) and mode I(b) failure separately.

  Predictions of mode II failure based on research on clamped plates is not valid for integral plates.

- Those theoretical solutions found to be valid for mode I failure for clamped plates are also valid for integral plates.

The theoretical prediction of Shen and Jones [5] for mode II failure in circular plates is shown to be valid for integral plates. The assumption of "fully clamped plates" used in [5] more accurately describes integral plates than clamped plates.

The predictions of Jones [6] and Olson et al [8] for mode II failure of square plates is not valid. In neither was shear considered.

It is concluded that shear plays a significant part in the rupture of thin plates subjected to impulsive loading.

The assumption of fully constrained edges does not accurately model the edge boundary conditions of clamped plates. Theoretical and numerical methods need to adjust the assumed boundary conditions to distinguish between clamped and integral plates.

8. RECOMMENDATIONS

Following the investigation and observations made during the investigations, the following recommendations are made:-

- The theoretical approach of Shen and Jones [5] has been shown to be valid for circular plates, and should be extended to include other plate geometries.

- The effect of thickness on the necking point and impulse required for rupture is not fully understood. More research is required. More experiments of the type used in this investigation, but with more variation in thickness and concentrating on impulses to rupture, could result in a better understanding of the mechanisms at work.

- The influence that shear plays in mode II failure needs to be investigated. Possibly by examining to effects of thickness.

- Finite element methods could be used to understand detail at the boundary of clamped plates by modelling the clamping and not just assuming a fixed boundary condition at the plate boundary.

REFERENCES

1. NURICK GN, MARTIN JB, 1989, **Deformation of thin plates subjected to impulsive loading - A review,** Int. J. Impact Engng. Vol.8, No.2, pp.159-186.

2. TEELING-SMITH RG, NURICK GN, 1991, **The deformation and tearing of thin circular plates subjected to impulsive loads,** Int. J. Impact Engng. Vol.11, No.1, pp.77-91.

3. NURICK GN, TEELING-SMITH RG, 1992, **Predicting the onset of necking and hence rupture of thin plates loaded impulsively - An experimental View,** Structures under shock and impact II, Computational Mechanics Publications, pp.431-445.

4. MARSHALL NS, 1992, **An investigation of the effects of boundary conditions on impulsively loaded plates,** Project No. 18a, Bsc, University of Cape Town.

5. SHEN WQ, JONES N, 1993, **Dynamic response and failure of fully clamped circular plates under impulsive loading,** Int. J. Impact Engng. Vol.13, No.2, pp.259-278.

6. JONES N, 1989, **Structural impact,** Cambridge University press.

7. JONES N, 1993, Private Communication.

8. OLSON MD, NURICK GN, FAGNAN JR, 1993, **Deformation and rupture of blast loaded square plates - Predictions and experiments,** Int. J. Impact Engng. Vol.13, No.2, pp.279-291.

9. JONES N, 1993, Private Communication.

10. NURICK GN, 1987, **Large deformations of thin plates subjected to impulsive loading,** Phd, University of Cape Town.

11. NURICK GN, SHAVE GC, 1994 , **The deformation and tearing of thin square plates subjected to impulsive loads - An experimental study,** (Submitted to Int. J. Impact Engng.)

BIBLIOGRAPHY

BODNER SR, SYMONDS PS, **Experiments on viscoplastic response of circular plates to impulsive loading**, J. Mech. Phys. Solids Vol.27, pp91-113.

DUFFEY TA, 1967, **The large deflection dynamic response of clamped plates subjected to explosive loading**, Sandia Laboratory, Albuquerque.

HUDSON GE, 1951, **A theory of the dynamic plastic deformation of a thin diaphragm**, J. Applied Physics, Vol.22, No.1, pp.1-11.

MENKES SB, OPAT HJ, 1973, **Broken beams**, Experimental Mechanics, November, pp.480-486.

PERRONE N, BHADRA P, 1984, **Simplified large deflection mode solutions for impulsively loaded, viscoplastic, circular membranes**, J. of Applied Mechanics Vol.51, pp. 505-509.

SYMONDS PS, WIERZBICKI T, 1979, **Membrane mode solutions for impulsively loaded circular plates**, J. of Applied Mechanics Vol.46, pp.58-63.

WANG AJ, HOPKINS HG, 1954, **On the plastic deformation of built-in circular plates under impulsive load**, J. of the Mech. and Physics of Solids, Vol.3, pp.22-37.

Appendix A

BALLISTIC PENDULUM

The pendulum geometry is shown in figure A.1 . The linearised equation of motion of the pendulum, assuming viscous damping, is :-

$$x''+2\beta x'+\omega_n^2 x \qquad \text{(A.1)}$$

where

$$\beta=\frac{C}{2M}$$
$$\omega_n=\frac{2\pi}{T}$$
$$\text{and}$$
$$\omega_d=(\omega_n^2-\beta^2)^{1/2}$$

and C is the damping coefficient, M is the total mass of the pendulum including the experimental rig, the balancing masses and the explosives, and T is the natural period of motion.

The solution of equation (A.1) is given by :-

$$x=\frac{e^{-\beta t}x_o'\sin\omega_d t}{\omega_d} \qquad \text{(A.2)}$$

where x_o' is the initial velocity of the pendulum.

Now, let x_1 be the horizontal displacement at $t = T/4$ and $-x_2$ be the displacement at $t = 3T/4$.

Substituting into equation (A.2) gives:-

$$x_1 = \frac{x_o' T e^{-\frac{1}{4}\beta T}}{2\pi} \qquad \text{(A.3)}$$

$$x_2 = \frac{x_o' T e^{-\frac{3}{4}\beta T}}{2\pi} \qquad \text{(A.4)}$$

Hence

$$\frac{x_1}{x_2} = e^{\frac{1}{2}\beta T}$$

which gives :-

$$\beta = \frac{2}{T} \ln \frac{x_1}{x_2} \qquad \text{(A.5)}$$

and

$$x_o' = \frac{2\pi x_1 e^{\frac{1}{4}\beta T}}{T}$$

The impulse can then be found from

$$I = M x_o' \qquad \text{(A.6)}$$

The period T is determined by taking the average of a number of measured pendulum oscillations with the mass being the same as that during testing. The damping constant ß is calculated from equation (A.5) where x_1 and x_2 are found from a number of pendulum oscillations in which the pendulum is held away from

the vertical and released a number of times.

It is clear from the pendulum geometry (fig. A.1) that the horizontal distanced moved by the pendulum, x_1, is not equal to the displacement recorded on the trace. This must be accounted for.

Consider figure A.1. When the pendulum is stationary, the horizontal distance from the end of the pendulum to the tip of the pen is given by

$$d_1 = (z^2 - a^2)^{1/2} \tag{A.7}$$

while at peak oscillations this distance decreases and is given by

$$d_2 = [z^2 - (a+y)^2]^{1/2} \tag{A.8}$$

The small oscillations of the pendulum during testing ensure that Θ is small enough that the assumption can be made that

$$x_1 \approx R\theta \quad and \quad y = \frac{R\theta^2}{2}$$

Therefore

$$y = \frac{x_1^2}{2R} \tag{A.9}$$

and

$$d^2 = [z^2 - (a + \frac{x_1^2}{2R})^2]^{1/2} \tag{A.10}$$

From figure A.1

$$x_1 = \Delta R + d_1 - d_2$$
$$\text{and}$$
$$x_2 = \Delta L - d_1 + d_2$$

Substituting for d_1 and d_2 gives

$$x_1 = \Delta R + (z^2 - a^2)^{1/2} - [z^2 - (a + \frac{x_1^2}{2R})^2]^{1/2} \qquad \text{(A.11)}$$

and

$$x_2 = \Delta L - (z^2 - a^2)^{1/2} + [z^2 - (a + \frac{x_1^2}{2R})^2]^{1/2} \qquad \text{(A.12)}$$

ΔL, ΔR, z, a and R are measured and therefore x_1 and x_2 can be calculated. Table A.1 gives all the constants of the ballistic pendulum during the experiments.

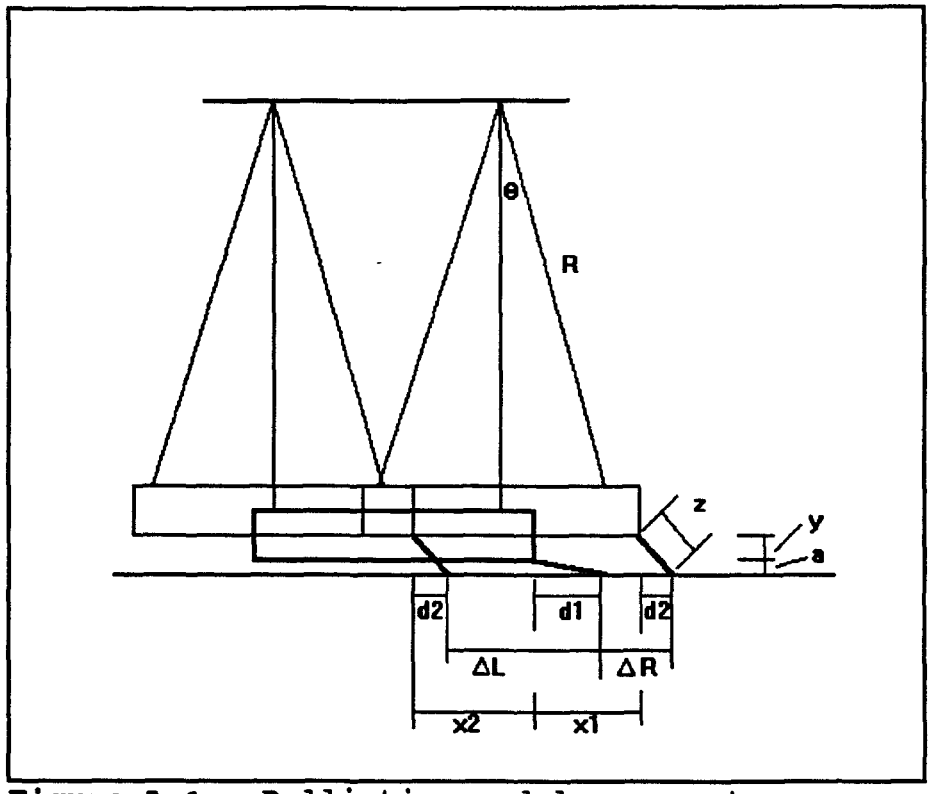

Figure A.1 - Ballistic pendulum geometry.

Table A.1 Ballistic Pendulum Details

R	-	2 550 mm
z	-	122 mm
a	-	53 mm
T	-	3.16 seconds
ß	-	0.011

Mass of test rig for Circular plates	-	82.9 kg
Mass of test rig for Circular plates with catch box	-	116.8 kg
Mass of test rig for Square Plates	-	82.4 kg

M = Mass of test rig + Mass of specimin

Typical pen stroke (dR) - 25 - 110 mm

Appendix B

PLATE THICKNESS

Circular Plates

The circular plates were measured at 13 positions over their surface. These values were averaged to give the thickness used in the analysis. The layout of the 13 positions where the plates were measured is shown in figure B.1.

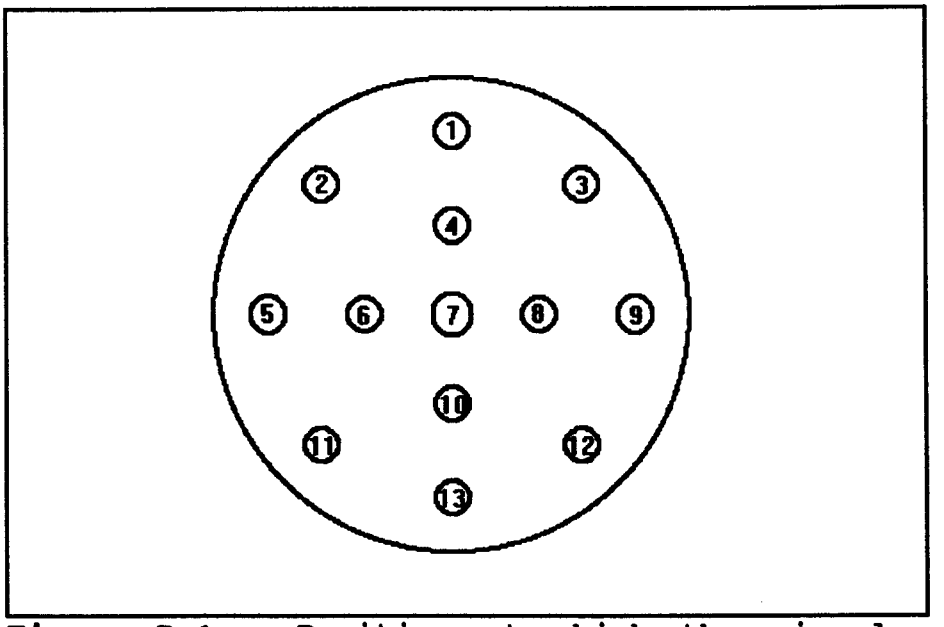

Figure B.1 - Position at which the circular plates were measured.

Test No.	Thickness at position (mm)							Average thickness	Mass
	1	2	3	4	5	6	7		
	8	9	10	11	12	13		(mm)	(kg)
22039301	1.68	1.68	1.68	1.68	1.66	1.66	1.65	1.658	4.74
	1.66	1.66	1.64	1.64	1.64	1.63			
22039302	1.70	1.68	1.71	1.69	1.67	1.67	1.67	1.684	4.76
	1.68	1.69	1.68	1.68	1.69	1.68			
22039303	1.85	1.85	1.85	1.85	1.86	1.84	1.84	1.848	4.86
	1.84	1.85	1.85	1.85	1.85	1.84			
22039304	1.68	1.69	1.67	1.66	1.69	1.67	1.65	1.675	4.85
	1.66	1.67	1.67	1.70	1.68	1.69			
22039305	1.73	1.74	1.74	1.74	1.75	1.74	1.73	1.745	4.81
	1.73	1.75	1.75	1.76	1.76	1.77			

22039306	1.63	1.63	1.63	1.63	1.61	1.63	1.63	1.629	4.76
	1.62	1.64	1.64	1.62	1.64	1.63			
22039307	1.63	1.63	1.64	1.63	1.62	1.60	1.61	1.629	4.81
	1.63	1.66	1.62	1.63	1.65	1.63			
22039308	1.77	1.77	1.78	1.77	1.77	1.77	1.76	1.779	4.71
	1.78	1.79	1.77	1.79	1.81	1.80			
22039309	1.52	1.53	1.53	1.53	1.55	1.54	1.54	1.544	4.84
	1.54	1.54	1.54	1.57	1.56	1.58			
22039310	1.77	1.77	1.77	1.75	1.77	1.76	1.74	1.760	4.77
	1.75	1.77	1.75	1.76	1.77	1.75			
22039311	1.78	1.78	1.78	1.77	1.76	1.76	1.75	1.769	4.89
	1.76	1.78	1.76	1.77	1.78	1.77			
23039301	1.59	1.59	1.58	1.56	1.58	1.58	1.55	1.575	4.80
	1.55	1.57	1.57	1.58	1.58	1.59			
23039302	1.70	1.70	1.71	1.71	1.71	1.71	1.70	1.713	4.86
	1.72	1.72	1.71	1.71	1.74	1.73			
23039303	1.75	1.77	1.75	1.74	1.76	1.75	1.73	1.747	4.86
	1.73	1.74	1.75	1.75	1.75	1.74			
23039304	1.65	1.65	1.65	1.65	1.64	1.64	1.64	1.645	4.86
	1.64	1.65	1.64	1.64	1.65	1.65			
23039305	1.73	1.72	1.72	1.70	1.70	1.70	1.68	1.696	4.85
	1.70	1.70	1.68	1.68	1.67	1.67			
23039306	1.95	1.97	1.96	1.96	1.99	1.98	1.95	1.972	4.65
	1.96	1.96	1.97	2.01	1.99	1.99			
23039307	1.61	1.62	1.60	1.59	1.60	1.57	1.57	1.583	4.85
	1.57	1.58	1.56	1.57	1.58	1.56			
23039308	1.70	1.70	1.70	1.68	1.70	1.68	1.67	1.695	4.76
	1.69	1.71	1.69	1.71	1.70	1.70			
23039309	1.74	1.75	1.76	1.75	1.76	1.77	1.75	1.769	4.74
	1.78	1.78	1.77	1.78	1.81	1.80			
23039310	1.74	1.74	1.74	1.74	1.74	1.73	1.73	1.739	4.70
	1.73	1.73	1.75	1.75	1.74	1.75			
2069301	1.60	1.60	1.61	1.59	1.60	1.60	1.58	1.597	4.75
	1.58	1.59	1.58	1.61	1.61	1.61			
2069302	1.73	1.73	1.71	1.72	1.73	1.72	1.71	1.717	4.76
	1.70	1.71	1.71	1.73	1.71	1.71			
2069303	1.75	1.76	1.76	1.75	1.77	1.76	1.74	1.761	4.88
	1.75	1.75	1.76	1.78	1.78	1.78			

2069304	1.54	1.55	1.56	1.51	1.55	1.53	1.51	1.541	4.77
	1.53	1.57	1.53	1.55	1.55	1.55			
2069305	1.65	1.65	1.63	1.63	1.64	1.60	1.60	1.627	4.77
	1.61	1.61	1.61	1.65	1.63	1.64			
2069306	1.60	1.60	1.59	1.59	1.59	1.59	1.59	1.595	4.80
	1.58	1.60	1.60	1.60	1.60	1.60			
2069307	1.72	1.74	1.73	1.70	1.74	1.72	1.71	1.727	4.75
	1.73	1.73	1.72	1.74	1.74	1.73			
2069308	1.53	1.57	1.60	1.57	1.58	1.57	1.57	1.582	4.78
	1.59	1.60	1.58	1.60	1.62	1.59			
2069309	1.75	1.74	1.74	1.73	1.75	1.75	1.74	1.748	4.73
	1.74	1.75	1.75	1.76	1.76	1.76			

Square Plates

The square plates were measured at 16 points on the plate. These points were equally spaced on a four by four grid.

Test No.	Thickness at measured points (mm)				Average Thickness (mm)	Mass (kg)
203931	1.66	1.66	1.66	1.66	1.66	4.739
	1.66	1.65	1.66	1.66		
	1.66	1.66	1.66	1.66		
	1.67	1.64	1.66	1.68		
203932	1.45	1.43	1.45	1.45	1.45	4.730
	1.45	1.43	1.44	1.46		
	1.44	1.45	1.44	1.46		
	1.46	1.46	1.46	1.47		
203933	1.65	1.65	1.66	1.65	1.64	4.740
	1.63	1.65	1.65	1.64		
	1.63	1.65	1.64	1.64		
	1.63	1.63	1.64	1.62		
803931	1.61	1.60	1.60	1.60	1.60	4.695
	1.61	1.60	1.60	1.60		
	1.61	1.60	1.59	1.60		
	1.61	1.60	1.60	1.60		

803932	1.54	1.54	1.55	1.56	1.55	4.713
	1.54	1.55	1.54	1.56		
	1.55	1.55	1.55	1.56		
	1.55	1.55	1.55	1.56		
803933	1.59	1.58	1.59	1.59	1.60	4.750
	1.60	1.59	1.59	1.59		
	1.61	1.59	1.61	1.60		
	1.62	1.62	1.61	1.62		
803934	1.66	1.65	1.65	1.64	1.65	4.845
	1.66	1.66	1.64	1.64		
	1.66	1.65	1.65	1.64		
	1.66	1.65	1.65	1.65		
803935	1.65	1.65	1.66	1.66	1.65	4.782
	1.66	1.65	1.64	1.66		
	1.64	1.63	1.63	1.65		
	1.64	1.64	1.64	1.64		
803936	1.64	1.62	1.62	1.60	1.62	4.777
	1.62	1.63	1.62	1.61		
	1.63	1.62	1.61	1.61		
	1.63	1.63	1.62	1.61		
803937	1.61	1.61	1.62	1.62	1.63	4.841
	1.61	1.62	1.63	1.63		
	1.63	1.63	1.63	1.63		
	1.63	1.63	1.64	1.64		
803938	1.58	1.58	1.58	1.59	1.59	4.693
	1.58	1.58	1.58	1.60		
	1.59	1.58	1.59	1.60		
	1.59	1.59	1.60	1.60		
803939	1.65	1.65	1.65	1.65	1.66	4.728
	1.66	1.66	1.65	1.65		
	1.66	1.66	1.66	1.66		
	1.67	1.67	1.67	1.67		
903931	1.64	1.63	1.62	1.62	1.62	4.831
	1.63	1.63	1.62	1.61		
	1.64	1.61	1.61	1.61		
	1.63	1.62	1.61	1.61		
903932	1.58	1.59	1.58	1.58	1.59	4.751
	1.59	1.61	1.61	1.59		
	1.60	1.58	1.59	1.59		
	1.60	1.59	1.59	1.59		

2069304	1.54	1.55	1.56	1.51	1.55	1.53	1.51	1.541	4.77
	1.53	1.57	1.53	1.55	1.55	1.55			
2069305	1.65	1.65	1.63	1.63	1.64	1.60	1.60	1.627	4.77
	1.61	1.61	1.61	1.65	1.63	1.64			
2069306	1.60	1.60	1.59	1.59	1.59	1.59	1.59	1.595	4.80
	1.58	1.60	1.60	1.60	1.60	1.60			
2069307	1.72	1.74	1.73	1.70	1.74	1.72	1.71	1.727	4.75
	1.73	1.73	1.72	1.74	1.74	1.73			
2069308	1.53	1.57	1.60	1.57	1.58	1.57	1.57	1.582	4.78
	1.59	1.60	1.58	1.60	1.62	1.59			
2069309	1.75	1.74	1.74	1.73	1.75	1.75	1.74	1.748	4.73
	1.74	1.75	1.75	1.76	1.76	1.76			

Square Plates

The square plates were measured at 16 points on the plate. These points were equally spaced on a four by four grid.

Test No.	Thickness at measured points (mm)				Average Thickness (mm)	Mass (kg)
203931	1.66	1.66	1.66	1.66	1.66	4.739
	1.66	1.65	1.66	1.66		
	1.66	1.66	1.66	1.66		
	1.67	1.64	1.66	1.68		
203932	1.45	1.43	1.45	1.45	1.45	4.730
	1.45	1.43	1.44	1.46		
	1.44	1.45	1.44	1.46		
	1.46	1.46	1.46	1.47		
203933	1.65	1.65	1.66	1.65	1.64	4.740
	1.63	1.65	1.65	1.64		
	1.63	1.65	1.64	1.64		
	1.63	1.63	1.64	1.62		
803931	1.61	1.60	1.60	1.60	1.60	4.695
	1.61	1.60	1.60	1.60		
	1.61	1.60	1.59	1.60		
	1.61	1.60	1.60	1.60		

803932	1.54	1.54	1.55	1.56	1.55	4.713
	1.54	1.55	1.54	1.56		
	1.55	1.55	1.55	1.56		
	1.55	1.55	1.55	1.56		
803933	1.59	1.58	1.59	1.59	1.60	4.750
	1.60	1.59	1.59	1.59		
	1.61	1.59	1.61	1.60		
	1.62	1.62	1.61	1.62		
803934	1.66	1.65	1.65	1.64	1.65	4.845
	1.66	1.66	1.64	1.64		
	1.66	1.65	1.65	1.64		
	1.66	1.65	1.65	1.65		
803935	1.65	1.65	1.66	1.66	1.65	4.782
	1.66	1.65	1.64	1.66		
	1.64	1.63	1.63	1.65		
	1.64	1.64	1.64	1.64		
803936	1.64	1.62	1.62	1.60	1.62	4.777
	1.62	1.63	1.62	1.61		
	1.63	1.62	1.61	1.61		
	1.63	1.63	1.62	1.61		
803937	1.61	1.61	1.62	1.62	1.63	4.841
	1.61	1.62	1.63	1.63		
	1.63	1.63	1.63	1.63		
	1.63	1.63	1.64	1.64		
803938	1.58	1.58	1.58	1.59	1.59	4.693
	1.58	1.58	1.58	1.60		
	1.59	1.58	1.59	1.60		
	1.59	1.59	1.60	1.60		
803939	1.65	1.65	1.65	1.65	1.66	4.728
	1.66	1.66	1.65	1.65		
	1.66	1.66	1.66	1.66		
	1.67	1.67	1.67	1.67		
903931	1.64	1.63	1.62	1.62	1.62	4.831
	1.63	1.63	1.62	1.61		
	1.64	1.61	1.61	1.61		
	1.63	1.62	1.61	1.61		
903932	1.58	1.59	1.58	1.58	1.59	4.751
	1.59	1.61	1.61	1.59		
	1.60	1.58	1.59	1.59		
	1.60	1.59	1.59	1.59		

903933	1.54	1.53	1.51	1.52	1.52	4.720
	1.52	1.53	1.51	1.51		
	1.53	1.52	1.51	1.51		
	1.53	1.52	1.51	1.51		
903934	1.47	1.46	1.46	1.47	1.47	4.716
	1.47	1.47	1.46	1.46		
	1.47	1.47	1.46	1.47		
	1.47	1.47	1.46	1.47		
903935	1.41	1.41	1.39	1.39	1.40	4.733
	1.40	1.39	1.40	1.39		
	1.40	1.39	1.40	1.39		
	1.42	1.40	1.40	1.40		
Not used	1.24	1.25	1.25	1.26	1.25	
	1.24	1.24	1.25	1.26		
	1.24	1.24	1.25	1.26		
	1.24	1.25	1.25	1.26		
Not used	1.28	1.29	1.29	1.29	1.29	
	1.29	1.28	1.29	1.30		
	1.29	1.29	1.29	1.30		
	1.29	1.29	1.29	1.30		
Not used	1.33	1.32	1.31	1.32	1.31	
	1.32	1.31	1.30	1.30		
	1.31	1.30	1.29	1.28		
	1.30	1.30	1.30	1.29		

Appendix C

Results of the Uniaxial Yeild Tests

Number	Strain Rate	Stress σ	Static stress σ_o	Strain to failure ϵ_f
	(s^{-1})	(MPa)	(MPa)	(%)
1	0.03347			
2	0.00033	281.37	256.65	35.18
3	0.00084	282.63	253.32	40.32
4	0.00167	291.17	257.02	35.97
5	0.00167	288.65	254.79	42.69
6	0.00084	303.67	272.18	39.92
7	0.00033	297.53	271.40	41.90
8	0.00017	296.14	273.23	40.32
9	0.00167	302.82	267.30	42.29
10	0.00084	275.07	246.55	42.29
11	0.00033	290.27	264.77	40.71
12	0.00017	269.42	248.58	45.85
13	0.00167	308.63	272.43	34.78
14	0.00084	344.16	308.48	41.50
15	0.00033	279.11	254.59	39.13
16	0.00017	286.12	263.99	38.74
21	0.00017	257.50	237.58	40.71
22	0.00033	277.21	252.86	39.92
23	0.00084	283.10	253.75	41.50
24	0.00167	***	***	41.11
Average value			261.64	40.25
Values used in calculations			262.0	40